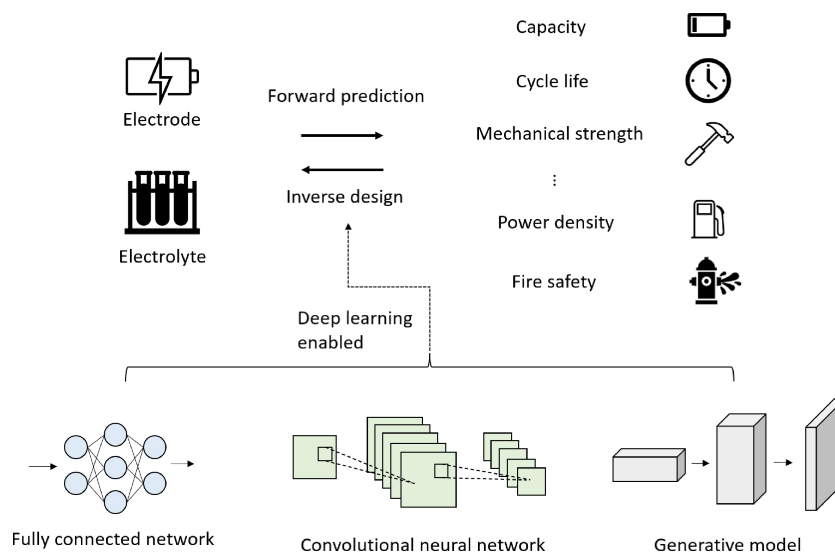


# Table of contents



Recent advancements in deep learning techniques offer promising solutions for the challenging task of optimizing batteries, particularly in improving electrodes and electrolytes. This review comprehensively explores the application of deep learning principles in addressing electrochemical problems related to batteries, bridging the gap between artificial intelligence and electrochemistry, and aims to inspire future progress in both scientific understanding and practical engineering in the field of battery technology.



# Designing electrodes and electrolytes for batteries by leveraging deep learning

Chenxi Sui<sup>1,§</sup>, Ziyang Jiang<sup>2,§</sup>, Genesis Higueros<sup>1,3,§</sup>, David Carlson<sup>2</sup> (✉), and Po-Chun Hsu<sup>1</sup> (✉)

<sup>1</sup> Pritzker School of Molecular Engineering, University of Chicago, Chicago, IL 60637, USA

<sup>2</sup> Civil and Environmental Engineering, Duke University, Durham, NC 27708, USA

<sup>3</sup> Thomas Lord Department of Mechanical Engineering and Materials Science, Duke University, Durham, NC 27708, USA

<sup>§</sup> Chenxi Sui, Ziyang Jiang, and Genesis Higueros contributed equally to this work.

Received: 27 July 2023 / Revised: 15 September 2023 / Accepted: 17 September 2023

## ABSTRACT

High-performance batteries are poised for electrification of vehicles and therefore mitigate greenhouse gas emissions, which, in turn, promote a sustainable future. However, the design of optimized batteries is challenging due to the nonlinear governing physics and electrochemistry. Recent advancements have demonstrated the potential of deep learning techniques in efficiently designing batteries, particularly in optimizing electrodes and electrolytes. This review provides comprehensive concepts and principles of deep learning and its application in solving battery-related electrochemical problems, which bridges the gap between artificial intelligence and electrochemistry. We also examine the potential challenges and opportunities associated with different deep learning approaches, tailoring them to specific battery requirements. Ultimately, we aim to inspire future advancements in both fundamental scientific understanding and practical engineering in the field of battery technology. Furthermore, we highlight the potential challenges and opportunities for different deep learning methods according to the specific battery demand to inspire future advancement in fundamental science and practical engineering.

## KEYWORDS

battery design, fast-charging battery, three-dimensional (3D) structure, deep learning, optimization

## 1 Introduction

To mitigate greenhouse gas emissions and air pollution, next-generation clean energy and sustainable fuels are urgent to be developed [1, 2]. Over the past few decades, renewable technologies such as hydropower, wind power, solar photovoltaics, and bioenergy have gained increasing significance in the quest for green electricity. According to a report, the power generated in the net zero scenario has increased from 19.8% to 28.7% between 2010 and 2021, with an ambitious goal of 60.9% in 2030 [3]. Furthermore, the global electric vehicle stocks have experienced significant growth, increasing from 11.3 million in 2010 to 2020, indicating a trend towards electrification for net zero emission transportation [4]. Additionally, industry-wide cost estimates for battery packs used in electric vehicles have decreased by approximately 14% annually between 2007 and 2014, from above US\$1,000 per kWh to around US\$410 per kWh, with the cost of battery packs used by market-leading battery electric vehicle (BEV) manufacturers even lower at US\$300 per kWh and declining by 8% annually [5]. These trends indicate a major transition towards renewable electricity, and electrochemistry is emerging as a powerful tool for energy and sustainability, with

applications ranging from energy storage [6–12], carbon capture [13–16], green energy generation [17–20], and smart buildings [21–26]. Among these technologies, battery plays an essential role in storing intermittent solar and wind energy for large-scale electrification [27–29].

The battery is a complex electrochemical system governed by chemical reactions, charge, and ion transport in solid and liquid phases, making it challenging to describe with simple physics formula [30]. Additionally, the electrode microstructures and electrolyte environment, including transfer number, conductivity, and viscosity, significantly impact the battery's performance in terms of charging and discharging rates, cycle life, and energy density. Although researchers have made significant progress in material synthesis through experiments and first-principle modeling, accurate and versatile prediction tools are urgently needed to explore optimal battery performance and reduce EV market prices under various scenarios, crossing large time and length scales and different application conditions.

The rapid development of deep learning (DL) algorithms has stimulated materials discovery by combining accurate first-principle simulations, autonomous synthesis, and testing

© The Author(s) 2023. Published by Tsinghua University Press. The articles published in this open access journal are distributed under the terms of the Creative Commons Attribution 4.0 International License (<http://creativecommons.org/licenses/by/4.0/>), which permits use, distribution and reproduction in any medium, provided the original work is properly cited.

Address correspondence to David Carlson, [david.carlson@duke.edu](mailto:david.carlson@duke.edu); Po-Chun Hsu, [pochunhsu@uchicago.edu](mailto:pochunhsu@uchicago.edu)

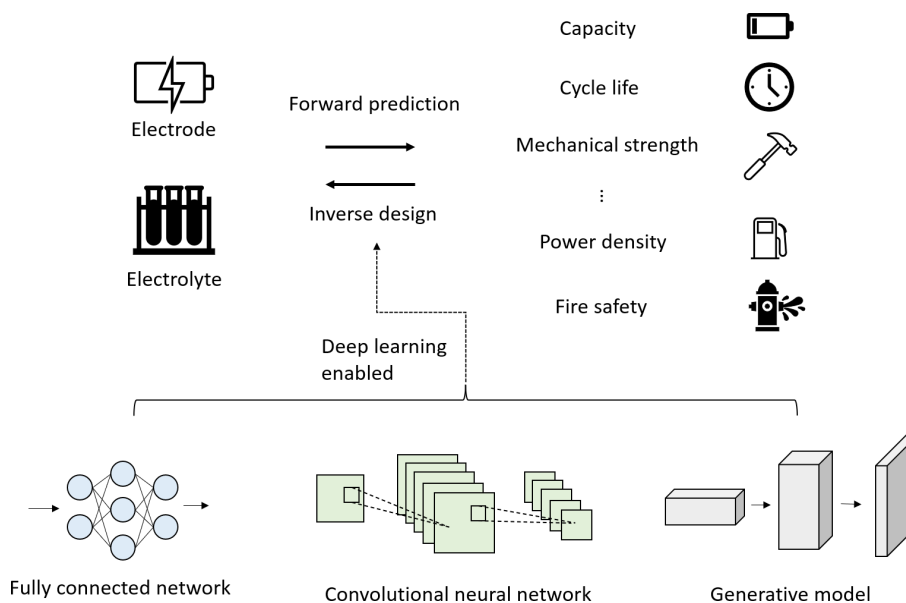


**Figure 1** Overview of deep learning enabled battery design.

experiments [31–44]. DL models can predict electronic, thermodynamic, and mechanical properties of the battery and its materials effectively, given a finite number of training datasets generated from experiments and/or simulations. In recent years, researchers have actively endeavored to explore the potential of DL in the field of battery design. In 2016, researchers started to apply DL techniques to predict the material properties of batteries, marking the inception of DL's role in battery design [45]. Then, within the materials science field, significant progress was made in advancing machine learning (ML) models to discover novel materials [40]. In the following years, especially 2019 and 2020, researchers developed and customized ML and data-driven methodologies to optimize fast-charging protocols and predict battery cycle life [46, 47]. The application of ML and DL became more diverse in battery research, with researchers delving into the analysis of battery structures [48], electrolytes [49], and their state-of-charge assessments [50]. A promising avenue for future research lies in the synergistic fusion of advanced characterization tools with artificial intelligence [51]. Indeed, integrating DL models into traditional experiments and simulations reduces the time and cost required for discovering and characterizing new electrode/electrolyte materials and additives for high-performance batteries, such as large capacity, high cycle life, strong mechanical strength, and improved safety. This contributes to the promising trend of electrification. In this review, we first elucidate basic algorithms in DL and then review recent applications of DL in electrode and electrolyte design (Fig. 1). We aim to bridge the gap between the battery design and artificial intelligence (AI) and inspire scientific and technological developments in materials science, computer science, and engineering to harness the battery's potential for sustainability.

## 2 Basic principles of machine learning and deep learning

We begin by offering a comprehensive overview of the fundamental principles and key concepts of commonly employed ML algorithms, spanning from simpler models like linear regression to more complex approaches such as probabilistic models and DL algorithms. Note that DL can be viewed as a

subset of ML, except that it employs structured frameworks such as neural networks and often relies on large input datasets for optimal performance. Subsequently, in Sections 3 and 4, we will delve into their applications in electrode and electrolyte design and conduct a comparative analysis with traditional design methods. It is important to highlight that while classification models play a crucial role in the field of ML, we will focus the discussion here on regression, which is common in battery design. Broader discussion of ML techniques are available elsewhere [52, 53].

### 2.1 Linear regression

We often begin modeling by assuming a linear relationship between the input features and targets before exploring nonlinear models. Suppose that we have a training set of independent input features  $\mathbf{X} = \{\mathbf{x}_1, \mathbf{x}_2, \dots, \mathbf{x}_N\}$  and target labels  $\mathbf{y} = \{y_1, y_2, \dots, y_N\}$ . The relationship between  $\mathbf{X}$  and  $\mathbf{y}$  is given as

$$y_i = \mathbf{w}^T \mathbf{x}_i + \varepsilon \text{ for } i = 1, 2, \dots, N \quad (1)$$

where  $N$  is the total number of samples in the training data,  $\mathbf{w}$  is a vector of parameters and  $\varepsilon$  is an unobserved noise (sometimes referred to as unexplained variability) term. When  $\mathbf{x}_i$  is multi-dimensional and  $y_i$  is one-dimensional, the method is referred to as multiple linear regression (MLR). Our objective is to estimate  $\mathbf{w}$  in such a way that the error between the predicted values  $\hat{y}_i$  and the target labels  $y_i$  is minimized on unseen data. It is worth noting that, for MLR, when we set the minimization objective to be the squared loss between the predicted values and the target labels, i.e.,  $\sum_{i=1}^N (y_i - \hat{y}_i)^2$ , this is equivalent to maximizing the likelihood function  $p(\mathbf{Y}|\mathbf{X}, \mathbf{w})$ , assuming that the noise  $\varepsilon$  follows a Gaussian distribution. Other linear methods, suggested as linear support vector regression [54], use alternative objective functions.

To make sure that the trained model generalizes to other data points which do not appear in the training set, we can add penalization terms on  $\mathbf{w}$ , leading to a penalized MLR (PMLR) model. PMLR models, such as ridge [55] or lasso [56] regression, have at least one setting (or “hyperparameter”) that must be chosen. Typically, this is chosen by randomly splitting all the available data into training, validation, and test datasets. The parameters are fit on the training data for a given set of hyperparameters and evaluated on the validation data. The

hyperparameters with the highest performance are chosen as the final model, and performance is evaluated on the test set to get an estimate of real-world performance. Model validation is critical for optimal scientific evaluation and should receive careful consideration.

### 2.2 Probabilistic algorithms

As described in Section 2.1, minimizing the squared error between the targets and predicted values is equivalent to maximizing the likelihood function so that the observed data is most probable, which gives us a point estimate for the parameters  $w$ . Instead, we may want to fully capture the posterior probability density  $p(w|X, y)$  to gain a comprehensive understanding of the parameter distribution and the model uncertainty (52). To achieve this, we assign a prior distribution on the model parameters and then use the observed data to update this prior. For example, to apply a Bayesian treatment on the multiple linear regression model in Section 2.1, instead of directly fitting the parameters  $w$ , we introduce a prior distribution over  $w$  and  $\epsilon$ :  $p(w|\alpha) = N(0, \alpha^{-1}I)$ ,  $p(\epsilon|\beta) = N(0, \beta^{-1})$ , where  $\alpha$  and  $\beta$  are precision parameters. Using the observed data  $D = \{X, y\}$ , we can calculate the posterior distribution  $p(w|D, \alpha, \beta) \propto p(D|w, \alpha, \beta)p(w|\alpha)$  and make inference on a new data point  $x^*$  via the predictive posterior below

$$p(y^*|x^*, D, \alpha, \beta) = \int p(y^*|x^*, D, w)p(w|D, \alpha, \beta)dw \quad (2)$$

which not only estimates the value of  $y^*$  but also gives an uncertainty estimate of the prediction. Such Bayesian treatments can be widely applied to many types of models.

A key relevant development from the Bayesian framework is the nonlinear and non-parametric approach called Gaussian process (GP), with which we define a prior distribution over functions and use the observed data to infer the posterior. Any finite number of random variables in a GP have a multivariate Gaussian distribution determined by the parameters of the GP [57]. A GP prior over a function  $f$  is completely specified by its mean function  $m(x) = \mathbb{E}[f(x)]$  and covariance function  $k(x, x') = \mathbb{E}[(f(x) - m(x))(f(x') - m(x'))]$

$$f(x) \sim GP(m(x), k(x, x')) \quad (3)$$

The covariance function defines the smoothness properties of the function. After fitting a GP, we can draw samples from the learned posterior distribution of functions evaluated at any number of inputs. In practice, GPs can be effectively utilized to incorporate prior information into functions or integrated with DL models to improve their predictive performance [58].

A typical application of GP is to serve as a surrogate model for Bayesian optimization when fine-tuning hyperparameters. This strategy offers greater efficiency compared to conventional hyperparameter tuning methods like grid search, as it dynamically determines the subsequent set of hyperparameters based on the model performance with respect to the preceding set [59, 60]. To give a concrete example, say we want to learn a function  $f: X \rightarrow Y$  to the observed data, i.e.,  $\hat{y} = f(x)$ , using a supervised learning model with hyperparameters  $\gamma$ . In most cases, hyperparameters are specified before training and we need to manually tune them if the model performance is unsatisfactory. Here, with Bayesian optimization, we treat  $\gamma$  as the input to a GP and the model performance  $s$  (e.g., performance on the validation data) as its output, i.e.,  $s(\gamma) \sim GP(0, k(\gamma, \gamma'))$ . After fitting the GP, for each  $\gamma$ , we can sample from this GP to obtain the mean performance

$\mu_s = \mu(\gamma)$  and its uncertainty  $\sigma_s = \sigma(\gamma)$ . We then use the acquisition function  $g$  on these values to determine an appropriate next set of hyperparameters to evaluate. A common choice of acquisition function is the upper confidence bound (UCB) as given below (some other popular acquisition functions include probability of improvement (PI) and expected improvement (EI))

$$g(\gamma; \lambda) = \mu_s + \lambda\sigma_s \quad (4)$$

where  $\lambda$  is an acquisition function parameter that controls the tradeoff between exploration and exploitation. Specifically, if  $\lambda$  is small, then  $g(\gamma; \lambda)$  will be dominated by  $\mu_s$ , meaning that we favor the solutions that have higher expected model performance. If  $\lambda$  is large, then  $g(\gamma; \lambda)$  will be dominated by  $\sigma_s$ , meaning that we prefer to explore the domains where we are uncertain about the model performance and might have higher performance. We determine the next set of hyperparameters by maximizing this acquisition function

$$\gamma_{next} = \underset{\gamma}{\operatorname{argmax}} g(\gamma; \lambda) \quad (5)$$

This process is repeated until we find the best set of hyperparameters  $\gamma^*$  which yields the best possible performance. This procedure can also be adapted to choose experimental settings in a wide array of contexts.

### 2.3 DL algorithms

The previously mentioned general ML algorithms depend heavily on the representations of the given data and are usually uncompetitive when the input  $x$  is intricate, such as image, audios, and videos [61]. To address this issue, instead of directly learning a mapping from the input space to the output space, it is necessary to learn the representation itself, and this is precisely where DL demonstrates its superiority. Over the past few decades, DL models have been extensively used in the field of computer vision [62–64], natural language processing [65–67], causal inference [68–72], healthcare [73–75], and environmental sciences [76–78].

#### 2.3.1 Multilayer perceptrons (MLPs)

MLP, or feedforward neural network (NN), is a commonly used DL models. MLP is a general ML method that also does not handle intricate data types, but we review it here as it forms the foundation of more complex DL approaches that take advantage of the structure of the more complex data types. It aims to learn a nonlinear functional mapping  $y = f_\theta(x)$  which maps an input vector  $x$  to an output representation  $y$ . Here  $\theta$  represents the

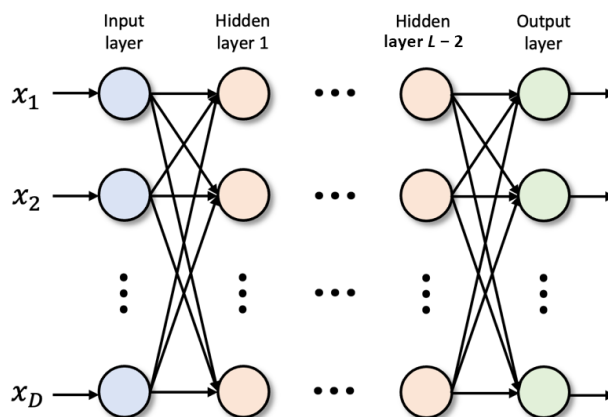


Figure 2 Architecture of a multilayer perceptron.

parameters of the neural network. A MLP with  $L$  layers is displayed in Fig. 2 below, where the network consists of an input layer, an output layer, and  $L - 2$  hidden layers.

As shown in Fig. 2, the input layer has the same number of units as the dimension of the input vector (i.e.,  $D$ -dimensional in this case). It takes in the input  $x$  and passes it to the first hidden layer. Each two consecutive hidden layers are connected by a set of weights and biases along with an activation function. Specifically, let us denote the  $i^{\text{th}}$  pre-activation and post-activation unit in the  $l^{\text{th}}$  layer as  $z_i^l$  and  $x_i^l$ , respectively. Also, we denote the weights and biases in the  $l^{\text{th}}$  layer as  $W_{ij}^l$  and  $b_i^l$ , respectively. We can compute  $z_i^l$  iteratively using Eq. (6)

$$z_i^l = b_i^l + \sum_{j=1}^{N_l} W_{ij}^l x_j^l, \quad x_i^l = \phi(z_i^{l-1}) \quad (6)$$

where  $N_l$  is the number of units in the  $l^{\text{th}}$  layer and  $\phi$  is a nonlinear activation function. As can be seen from the equation above,  $W_{ij}^l$  and  $b_i^l$  define an affine transformation between the  $(l-1)^{\text{th}}$  and the  $l^{\text{th}}$  layers. In the absence of  $\phi$ , the MLP would just be a sequence of affine transformations which is not capable of capturing nonlinear functional relationships, underscoring the necessity of nonlinearity. Some frequently used nonlinear activations include the rectified linear units (ReLU) [79], leaky ReLU [80], and hyperbolic tangent (tanh) [81]. The selection of the activation function for the output layer is typically dependent on the specific task at hand. For instance, the identity function may be used for regression, the sigmoid function for binary classification, and the softmax function for multi-class classification. The size of the output layer is also dependent on the task at hand; in the case of a single regression prediction, there would only be a single output unit.

The training process of neural networks is similar to that of the linear regression models as we have discussed in Section 2.1. For example, we can learn the neural network parameters  $\theta$  to maximize the likelihood function  $p(\mathbf{X}, \mathbf{Y}|\theta)$ , which is equivalent to minimizing a squared error for regression or a cross-entropy error for classification. Gradient-based methods, including mini-batch gradient descent and stochastic gradient descent, are often used to optimize the neural network parameters with respect to the loss function by back-propagating the gradients [82]. It is

important to highlight that the nonlinearity in neural networks gives rise to a nonconvex loss surface; however, in practice gradient methods find good solutions on the loss surface [82].

### 2.3.2 Convolutional neural networks (CNNs)

CNNs [83, 84] are a well-established class of DL models, widely recognized for their ability to effectively process complex input data with multiple channels (e.g., audios, images, and videos). Standard CNNs usually include two types of operations: convolution and pooling. These convolution and pooling operations are designed to take account of structure in the data, such as the common structures in images. These operations allow CNNs to drastically outperform MLPs in many types of data, and CNNs form the foundation of top performing computer vision models. An example of two-dimensional (2D) convolution layer is shown in Fig. 3 below.

In the figure depicted above, the input and kernel (or filter) of the convolutional layer are represented by  $\mathbf{X}$  and  $\mathbf{w}$ , respectively. Notably, the size of the kernel is typically smaller than that of the input, resulting in partial connectivity between each output unit and the input units. This design choice significantly reduces the computational cost and enables the CNN to extract meaningful features from small sub-regions of the input.

The pooling operation, on the other hand, applies a summary statistic (e.g., maximum and average) to each sub-region of the input by sliding a kernel (or filter) with a certain stride size, resulting in an output with reduced dimensions compared to the input. Pooling introduces local invariance properties to the output, including translational and rotational invariance. Translational invariance is achieved because the pooling operation is applied independently to each sub-region, allowing it to detect the same features regardless of their position within the sub-region. Rotational invariance is a consequence of the pooling operation being insensitive to the orientation of the features within the sub-region. These local invariance properties make the output more robust to small changes in the input, improving the generalization performance of the CNN.

### 2.3.3 Recurrent neural networks (RNNs)

RNNs [82, 85] are a family of DL models for processing sequential data such as time series and text streams. The hidden units in

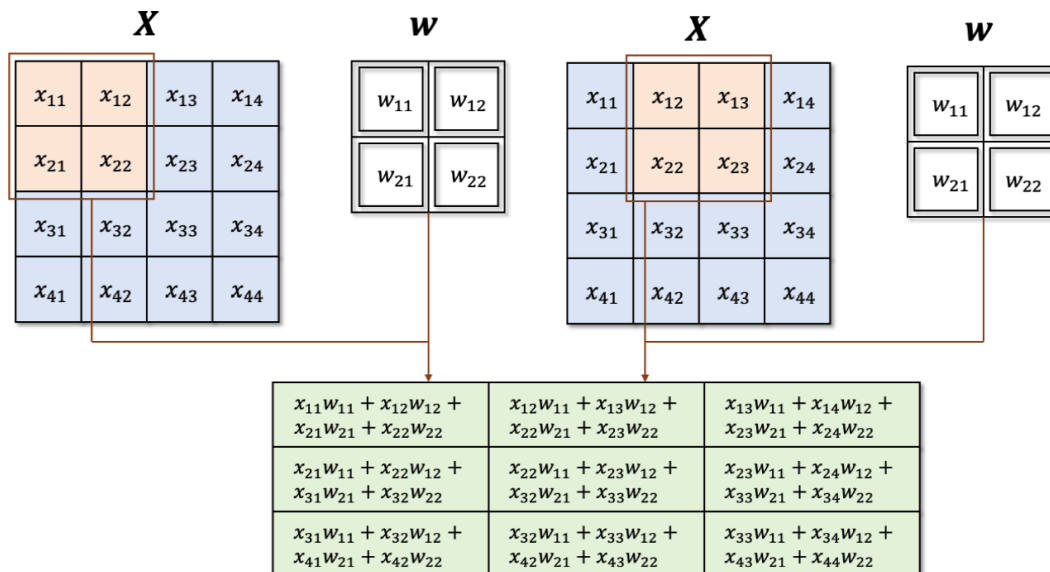
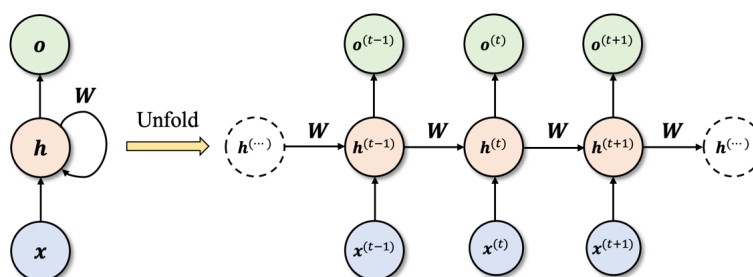


Figure 3 An example of 2D convolution layer with a kernel size of  $2 \times 2$ .



**Figure 4** Computation graph of a fully recurrent neural network.

RNNs are usually referred to as states (denoted as variable  $\mathbf{h}$ ). The computational graph, both before and after unfolding, of a fully RNN (FRNN) is illustrated in Fig. 4, where each output unit  $\mathbf{o}^{(t)}$  at time step  $t$  is connected to each input unit  $\mathbf{x}^{(t)}$ . This connectivity enables the network to retain and utilize information from all previous time steps, allowing it to capture temporal dependencies and patterns in the input data. The training procedure for RNNs is relatively straightforward, as the gradients are propagated backward along the unfolded computation graph. This algorithm is commonly known as backpropagation through time (BPTT) [86].

One of the significant challenges associated with RNNs is their inability to handle long-term dependencies when the unfolded computational graph becomes extremely deep. Specifically, the forward pass of an RNN involves repeatedly applying the same affine transformation and a nonlinearity, as depicted in Fig. 4, the gradient may either vanish or explode, rendering the RNN difficult to train. The vanishing gradient problem occurs when the gradient becomes extremely small, making it difficult for the network to learn from past information. On the other hand, the exploding gradient problem occurs when the gradient becomes exceedingly large, making the network learning unstable.

Several techniques have been proposed to address the vanishing and exploding gradient problem in RNNs. For instance, gradient clipping can prevent the gradient from exploding, while parameter regularization can help with the vanishing gradient issue. One of the most notable solutions is the introduction of the long short-term memory (LSTM) model by Hochreiter and Schmidhuber [87]. The LSTM model allows the RNN to learn whether to remember or forget relevant information using gated memory cells, making it particularly well-suited for processing long sequences of data. Another variant of the LSTM model is the gated recurrent unit (GRU), which has a simpler structure but performs comparably well to LSTM [88, 89].

Despite these advances, recent developments in ML have shown that attention mechanisms [90] and transformer architectures [67] outperform RNNs in many cases. Attention mechanisms allow for modeling dependencies between different parts of a sequence without regard to their distance in the input or output sequences. The transformer architecture, which is based solely on attention mechanisms and does not use recurrent connections, has achieved state-of-the-art results in many natural language processing and computer vision tasks. Therefore, while RNNs continue to be a valuable tool for ML applications, attention-based models have emerged as a promising alternative for modeling sequential data.

### 2.3.4 Deep generative models

Unlike regression-based models or conventional neural networks that directly estimate the conditional probability of the target

variable given the input, i.e.,  $p(y|\mathbf{x})$ , generative models estimate the joint distribution  $p(\mathbf{x}, y)$  on both the input and the target variable (or just the data  $p(\mathbf{x})$ ). Many deep generative models are based on modifying the structure an autoencoder (AE), which is a neural network comprising an encoder function  $\mathbf{z} = f(\mathbf{x})$  that maps the input  $\mathbf{x}$  into a latent feature  $\mathbf{z}$  and a decoder function  $\hat{\mathbf{x}} = g(\mathbf{z}) = g(f(\mathbf{x}))$  that reconstructs the input  $\mathbf{x}$ .  $f(\cdot)$  and  $g(\cdot)$  are defined as neural networks, and can easily use MLPs or CNNs (for a deep convolutional AE [91]). In practice, AEs have been successfully applied to many tasks including dimensionality reduction, representation learning, and information retrieval, but are not natural generative models without modification.

One extension to form a deep generative model is the variational AE (VAE) framework of Kingma and Welling [92]. The VAE defines the latent feature  $\mathbf{z}$  as an unobserved continuous random variable with a prior distribution  $p(\mathbf{z})$ . The observed variable  $\mathbf{x}$  is then generated from a conditional distribution  $p(\mathbf{x}|\mathbf{z})$ , which is defined by adding a distribution to the decoder, such as  $\mathbf{x} \sim N(g(\mathbf{z}), \sigma^2 I)$  ( $I$  is the identity matrix). However, computing the marginal distribution  $p(\mathbf{x}) = \int p(\mathbf{x}|\mathbf{z})p(\mathbf{z})d\mathbf{z}$  is typically infeasible, which also makes the posterior of the latent variable  $p(\mathbf{z}|\mathbf{x}) = p(\mathbf{x}|\mathbf{z})p(\mathbf{z})/p(\mathbf{x})$  computationally intractable. Thus, the VAE introduced a variational Bayes approach to optimize an approximation of the posterior,  $p(\mathbf{z}|\mathbf{x}) \approx q(\mathbf{z}|\mathbf{x}) = N(f(\mathbf{x})_{\mu}, \text{diag}(f(\mathbf{x})_{\sigma^2}))$ , meaning that the encoder estimates both the mean and the variance of the posterior approximation. This framework can be trained using the evidence lower bound objective common in variational Bayes [92].

An alternative deep generative model is the generative adversarial network (GAN) [93] that consists of two models: a generator  $f_g(\mathbf{z}; \theta_g)$ , which maps an input noise variable  $\mathbf{z}$  into the data space, and a discriminator  $f_d(\mathbf{x}; \theta_d)$ , which evaluates whether an input  $\mathbf{x}$  comes from real data or from the generator by outputting a probability  $0 \leq f_d(\mathbf{x}) \leq 1$ . Here  $\theta_g$  and  $\theta_d$  represents the parameters of the generator and the discriminator, respectively. The generator and discriminator models are trained concurrently in an adversarial minimax game until the generator produces samples that cannot be distinguished from real data by the discriminator. Specifically,  $f_g$  and  $f_d$  are optimized by playing the following minimax game with value function  $V(f_g, f_d)$

$$\min_{f_g} \max_{f_d} V(f_d, f_g) = \mathbb{E}_{\mathbf{x} \sim p_{\text{data}}(\mathbf{x})} [\log f_d(\mathbf{x})] + \mathbb{E}_{\mathbf{z} \sim p(\mathbf{z})} [\log (1 - f_d(f_g(\mathbf{z})))] \quad (7)$$

Given arbitrary functions  $f_g$  and  $f_d$ , it is theoretically established that, under reasonable assumptions,  $f_g$  will recover the original data distribution [93, 94]. The applications of GAN are diverse, including image synthesis, style transfer, image-to-image translation, and text-to-image generation.

Additionally, the diffusion model [64, 95] represents another

type of deep generative model that has gained increasing popularity. However, the diffusion model as it has not been extensively used for electrode and electrolyte design. Nevertheless, we acknowledge its potential as a promising direction for future research in this domain.

Together, VAEs, GANs, and diffusion techniques are now fundamental tools that are helping to power the current generative AI revolution [96].

### 3 Deep learning-assisted electrode design

Developing fast-charging batteries is critical for the electrification of transportation to mitigate carbon emissions and climate change. The U.S. Department of Energy has set an ambitious goal of enabling electric vehicles to recharge under 10 min, covering a distance of 200 miles [28, 97]. This objective presents significant challenges and opportunities for scientists and engineers to overcome conventional obstacles in different aspects and scales. The main hurdle is balancing the battery's capacity and charging rate. Most batteries struggle to maintain high capacity when charged quickly due to the mass transport limitation and the ineffective utilization of deep electrode materials. Addressing this issue requires rational designs of the electrode microstructures and materials. However, with increasing resolutions of electrode design and characterization, more complex datasets are generated, leading to a need for advanced analysis techniques to extract detailed insights about samples. As a result, DL models become viable tools to assist in the analysis and deduction of complex datasets and parameters space and bridge the gap between experimental data and multiphysics modeling.

#### 3.1 Governing physics and traditional methods

Within battery systems, the solid-state matrices (or active materials) play a crucial role in facilitating the transport of electrons, and the electrolyte is responsible for enabling the flow of ions between the positive and negative electrodes. However, the tortuous path of the porous electrode, due to the randomly packed

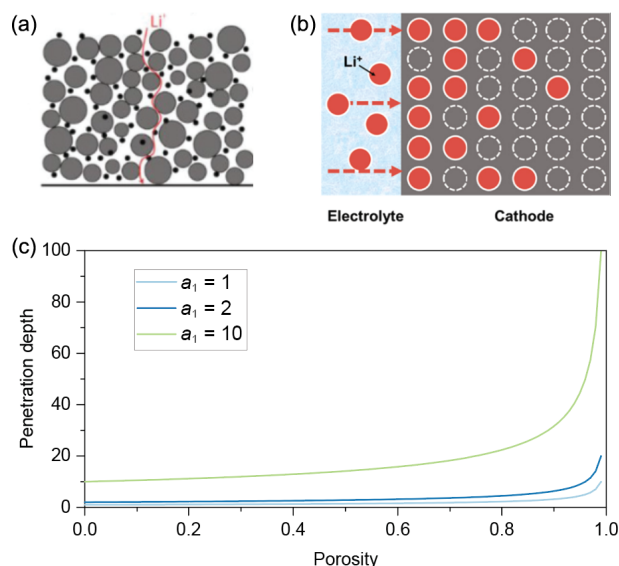


**Figure 5** Key challenges of ionic transport in porous electrodes under fast-charging. (a) High tortuosity in the traditional porous electrode. Reproduced with permission from Ref. [99], © WILEY-VCH Verlag GmbH & Co. KGaA, Weinheim 2018. (b) Non-uniform ions distribution in the porous electrode. Reproduced with permission from Ref. [100], © American Chemical Society 2022. (c) Penetration depth as the function of porosity.

particles, can hinder the ionic transport, resulting in elevated resistance and a reduction in battery performance (Fig. 5(a)). Thus, the degree of turning of the ionic path in a porous electrode is defined as its tortuosity ( $\tau$ ). This parameter is crucial as it directly impacts capacity under high current density. The tortuosity can be mathematically represented as

$$\tau = \varepsilon \frac{D_0}{D_{\text{eff}}} \quad (8)$$

where the  $\varepsilon$  is the overall porosity of the porous electrode,  $D_0$  is the diffusivity of electrolytes, and  $D_{\text{eff}}$  is the effective diffusivity of the ions through the whole porous electrode. In general, an elevated level of tortuosity results in increased ion transport resistance, thereby negatively affecting the performance of the battery. Conversely, a lower degree of tortuosity promotes faster ion transport, which enhances the battery's overall performance and its efficiency. In other words, tortuosity is an essential problem that needs to be solved for porous electrodes.

In addition to tortuosity, the reaction rate distribution is another essential factor governing electrochemical kinetics. The nonlinearity of the Nernst–Planck equation causes a significant gradient in ionic concentration and reaction rate along the depth of the electrode. These gradients lead to poor utilization of deep (far from the separator) electrode materials when attempting to improve energy and power density via thick electrodes (Fig. 5(b)). This non-uniform distribution is highly dependent on the electrode's porous structures. To elucidate this phenomenon, we introduce a physical term called “reaction penetration depth” based on John Newman's theory for a one-dimensional (1D) porous electrode [98]. This theory simplifies the three-dimensional (3D) partial differential equation groups to a 1D form. If we solve equations by inserting boundary conditions and physical assumptions, we can get a relationship between the reaction penetration depth (PD) and the porosity of the electrode

$$\text{PD} = a_1 \sqrt{\frac{1}{1 - \varepsilon}} \quad (9)$$

where  $a_1$  is the constant related to materials properties (i.e., electronic and ionic conductivity and size of active materials particles) and  $\varepsilon$  is the porosity of the electrode. The equation indicates that increasing the electrode porosity can facilitate deeper reaction penetration, resulting in improved specific capacity during high C-rate charging. Figure 5(c) demonstrates the improvement of penetration depth through an increase in average porosity. Varying  $a_1$ , or the material properties, implies that this penetration depth relationship applies to different electrode materials and electrolytes. Hence, to enhance the performance of the battery during fast-charging, it is crucial to develop an optimal electrode structure and select suitable materials to balance out the gradient distribution of the reaction rate and alleviate the effects of tortuosity.

Significant process has been made to improve the battery fast-charging performance by designing the microstructures and materials. Ramadesigan et al. first tried to solve the gradient issue theoretically by optimizing the local porosity of the electrode along the depth [101, 102]. It was observed that gradual porosity across the electrode in an optimal manner for a specific amount of active material can result in a 15%–33% reduction in the ohmic resistance. In lithium-ion battery design, single objective optimization such as reducing overall electrode resistance through a graded design has a modest effect of 4%–6%. Multiple objective optimizations, such as resistance and overpotential variance,

allows for a broader design space to achieve multiple goals. Then, inspired by theoretical progress, Liu et al. developed a bilayer electrode with gradual porosity [103]. Their research showed that gradual porosity can decrease capacity fade by about 8.285% in full cell and 5.29% in half-cell. The increase in porosity enhances the conductivity and diffusivity of lithium-ions in the electrode and allows for control of solid electrolyte interphase (SEI) formation. Additionally, Zhao et al. introduced a gradient electrode design with vertically aligned porous channels that have smaller openings on one end and larger openings on the other [104]. It is found that faster kinetics occur in larger openings with more concentrated active material near the separator. Similarly, Huang et al. employed the ice templating technique to produce thick cathodes (with a thickness of 900  $\mu\text{m}$ ) based on  $\text{LiFePO}_4$ . The cathodes were designed to have a pore structure gradient and fast ion transport pathways, which enable high energy densities at fast rates [105]. Furthermore, Kim et al. also created stratified electrodes with  $\text{Li}[\text{Ni}_{0.6}\text{Co}_{0.2}\text{Mn}_{0.2}]\text{O}_2$ , which improved the cycle life [106].

Low-tortuosity or graded porosity electrodes can also be fabricated by sacrificial template method (Fig. 6). The designed pore structures form after the templates in the slurry are removed. Bae et al. used co-extrusion to produce templates and thus macro-pore channels, with controlled channel spacings. The resulting

low-tortuosity electrodes have tunable channel spacing down to  $\sim 15 \mu\text{m}$  and showed 3 times areal capacity under 2 C charging rate [107]. Sander et al. utilized magnetic field to align the sacrificial templates to create low-tortuous electrodes. The magnetic field can not only align the magnetized nylon rod, but also the magnetic emulsion droplets [108]. Billaud applied a similar method and showed the enhanced ionic transport in the battery [109]. Zhang et al. also combined the magnetic alignment and ice-template method for low-tortuous electrode fabrication. Under 10  $\text{mA}/\text{cm}^2$ , the electrodes exhibit an areal capacity of approximately 3.6  $\text{mAh}/\text{cm}^2$  [110]. Despite the notable advancements achieved by physics-guided research, a gap remains in attaining the optimal structure in various application scenarios.

### 3.2 Deep learning method and results

It is apparent that the future of electrode design is heavily linked to the development of DL, given the challenges of identifying optimal structures for diverse application scenarios in complex parameter spaces. Employing DL across the materials synthesis, structure design, and characterization can significantly enhance design efficiency and accuracy. In this section, we will discuss recent progress in DL-assisted electrode optimization and analysis.

As mentioned earlier, one of the significant challenges in battery design is the slow ionic transport in porous electrodes.

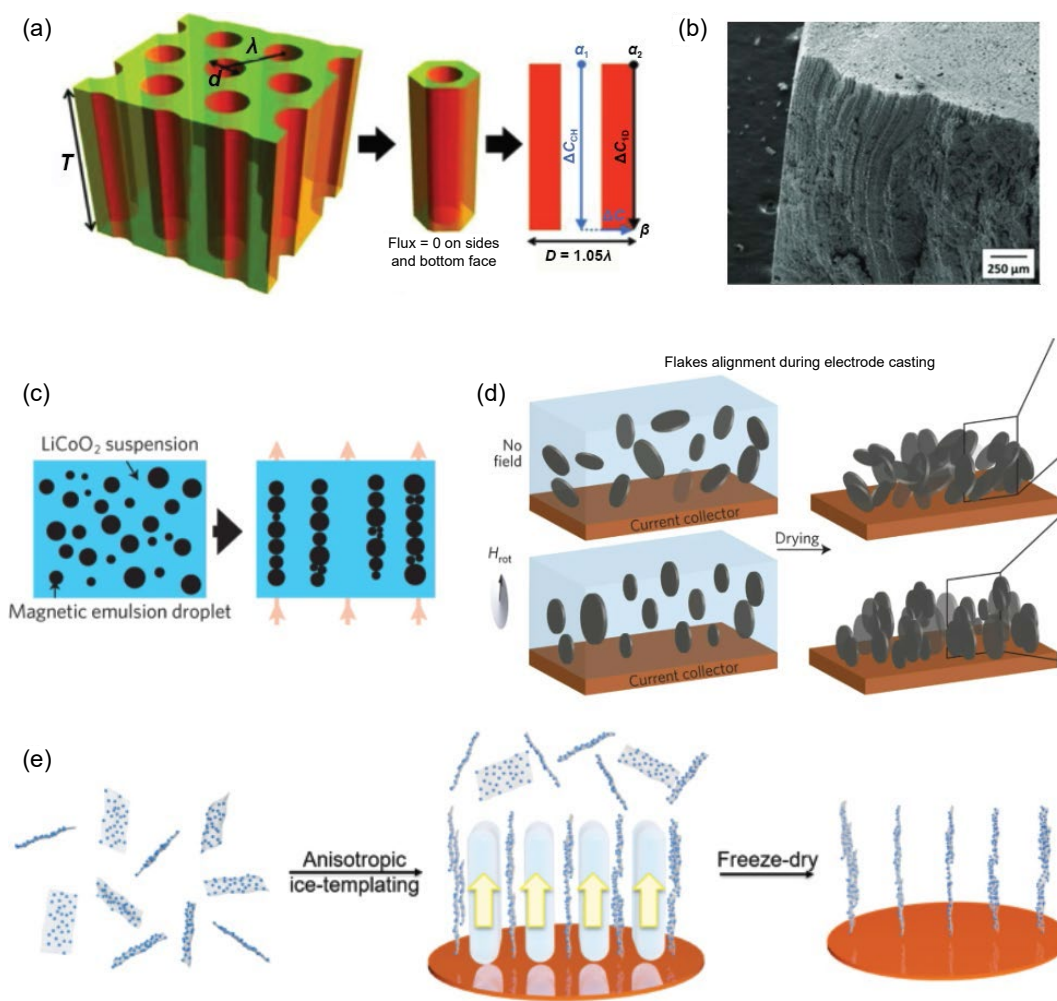


**Figure 6** Low-tortuous electrodes fabrication. (a) Low-tortuous channels in the electrodes and geometric control factors. (b) SEM image of the fabricated electrode. (a) and (b) Reproduced with permission from Ref. [107], © WILEY-VCH Verlag GmbH & Co. KGaA, Weinheim 2013. (c)–(e) Creating the low-tortuous channels by magnetic field alignment method and ice-template method. Reproduced with permission from Ref. [108], © Macmillan Publishers Limited, part of Springer Nature 2016; Ref. [109], © Macmillan Publishers Limited, part of Springer Nature 2016; Ref. [110], © American Chemical Society 2019.

While progress has been made in designing low-tortuosity batteries through vertical channels and gradient active materials [107–110], optimal solutions have yet to be found. Although topological optimization has been applied to search for suitable electrode structures, time-dependent charging problems and the time-consuming nature of solving 3D finite element models remain obstacles [111]. To address these issues, Sui et al. drew inspiration from nature and introduced efficient vascular channels into the porous electrode to enhance ionic transport and mitigate non-uniform reaction rate distribution [97]. The vertical central channels and gradient branch channels reduced tortuosity and increased reaction penetration depth. Given the large number of possible vascular channel designs, Sui et al. developed a DL pipeline to accelerate computation speed (Fig. 7). The neural network, informed by the geometric factors of the electrode, speeded up computation for all possible electrode designs and corresponding charging curves by 84 times, compared to the conventional finite element method. Furthermore, they developed an inverse design workflow to find the optimal electrode structure from the total library of computed designs under different application scenarios, such as varying charging rates. The workflow delivered a customized package containing electrode geometric factors, charging curves, charging capacity, and energy density. With the aid of bio-inspired vascularized design and DL-based prediction, the optimized porous electrode demonstrated a

66% improvement in capacity under 3.2 C constant current charging. This work can potentially inspire advancements in the experimental and theoretical aspects of fast-charging batteries in the future.

Besides, GANs and CNNs can also be used to design the microstructure in the electrodes. Niu et al. proposed a performance-informed learning framework, called  $\pi$  learning, to generate electrode microstructures informed by electrochemical performance [112]. This is achieved by integrating GANs and deep NNs with physical knowledge to accurately predict current density. The framework was demonstrated in two design philosophies, inverse and forward design, for solid oxide fuel cell (SOFC) anodes. The results showed that  $\pi$  learning can generate electrode microstructures with the globally optimal electrode microstructure. The physical and electrochemical insights obtained by prediction can guide the rational design of SOFC electrodes. The framework can be easily transferred to the design of other porous electrodes in various electrochemical devices, such as fuel cells and batteries.  $\pi$  learning can be further enhanced by involving high-dimensional multi-physics computation to inform the generative model (Fig. 8(a)).

In addition to electrode design, characterization is a crucial tool for understanding physical mechanisms and evolution to advance the design of batteries. The performance of batteries depends on the transport of lithium ions and the kinetic process of electrodes,

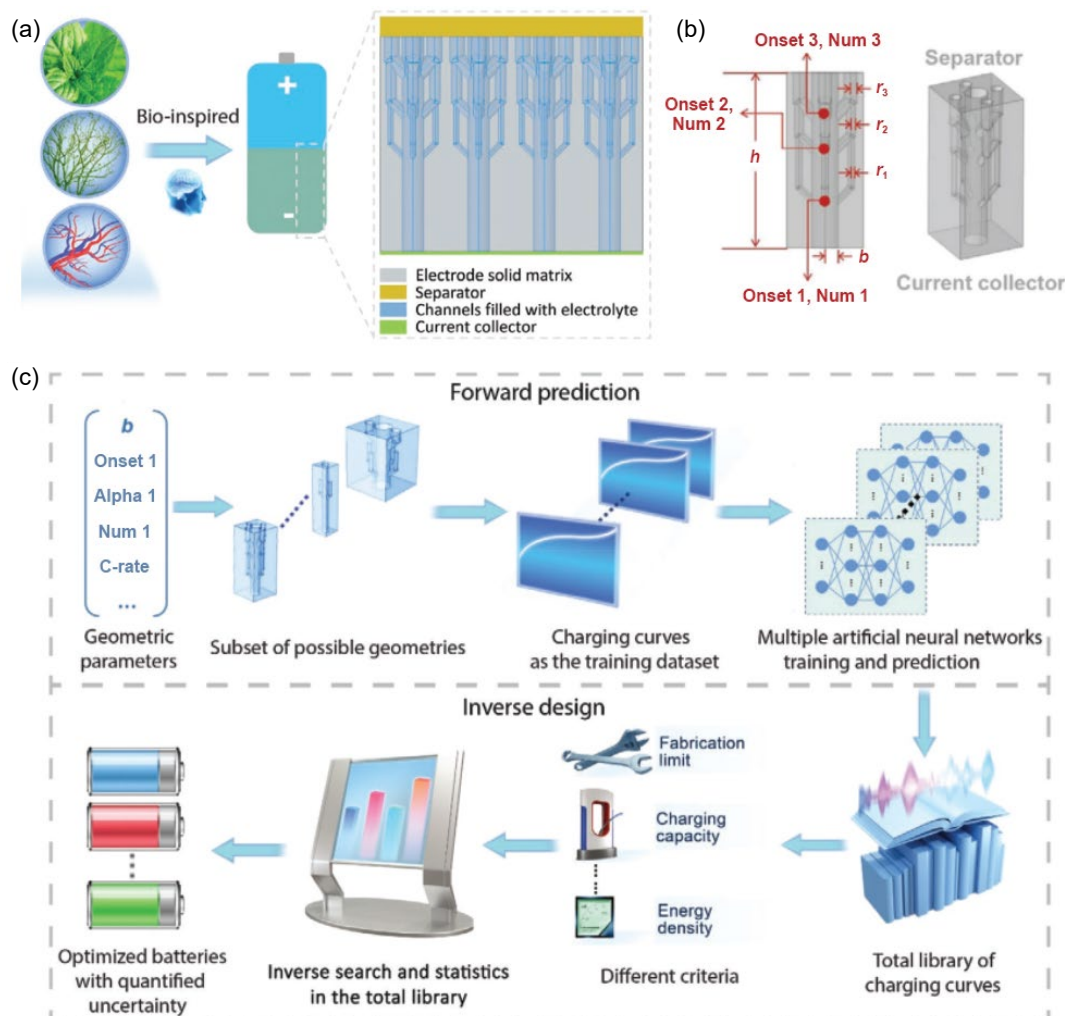


**Figure 7** Bio-inspired vascularized electrode designed by deep learning. (a) Bio-inspired concept. (b) Geometric factors of vascular electrodes. (c) Deep learning optimization loop. Reproduced with permission from Ref. [97], © Wiley-VCH GmbH 2021.

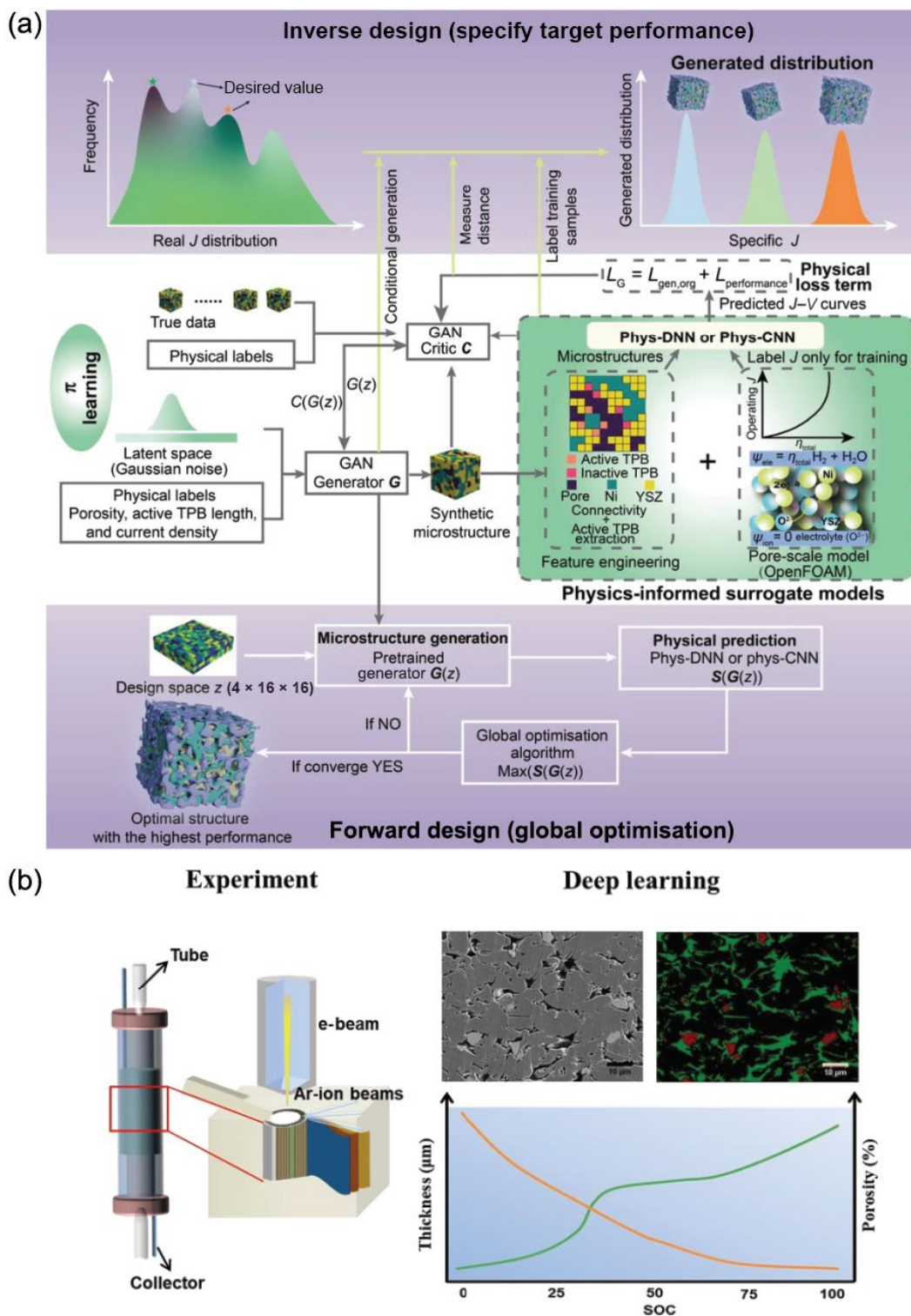


**Figure 8** Deep learning assist microstructure of electrode design and characterization. (a)  $\pi$  learning for electrode microstructure design. Reproduced with permission from Ref. [112], © Niu, Z. Q. et al. 2023. (b) Electrode microstructure characterization with the help of deep learning. Reproduced with permission from Ref. [117], © Yang, Y. Z. et al. 2022.

which are influenced by microstructure parameters such as porosity and tortuosity. These parameters play a vital role in predicting the fast-charging performance. Visualizing electrode microstructure during the service process is imperative for optimizing electrode structure and diagnosing potential safety issues. Fortunately, significant progress has been made in the field of picture processing and complex structure analysis, providing a robust framework for electrode microstructure visualization and

analysis [113–116]. Yang et al. studied the evolution of electrode microstructure in a battery by using a modified U-Net CNN for high-precision segmentation (Fig. 8(b)) [117]. DL is used to obtain the porosity and thickness of the negative and positive electrodes at different states of charge, and the relationship between the evolution of porosity and thickness during charging. The method could be extended to measure additional microstructural parameters using broad ion beam-scanning electron microscopy

(SEM)/focused ion beam (FIB)-SEM for 3D models in the future, providing an approach to exploring microstructure evolution and aiding in electrode structure optimization. Additionally, Gayon-Lombardo presented a method for creating synthetic three-dimensional microstructures consisting of several material phases using deep convolutional GANs (DC-GANs). This approach enables the model to represent the statistical and morphological characteristics of actual microstructures. The study used two open-source microstructural datasets, and various microstructural properties were calculated for the real data and compared to the synthetic structures created by the trained generator. The results showed excellent agreement, although the synthetic structures had a smaller variance than the training data [118]. Moreover, Petrich et al. developed a classifier that distinguishes between three causes for particle separation using the shape of the gap between particles [119]. Simulated anode material was used to generate correctly labeled sample data for developing the classifier. The classifier was then tested using hand-labeled data from a real electrode, achieving an overall accuracy of 73%.

#### 4 Deep learning-assisted electrolyte design

In addition to the electrode, electrolyte is another crucial component that significantly affects the performance of batteries. Electrolyte plays a vital role in facilitating ion transport in rechargeable batteries. However, the design of electrolytes for fast-charging batteries poses a significant challenge. Unlike solid electrodes, electrolytes are highly disordered, making it difficult to identify the governing physical factors and optimize their properties. Additionally, the vast number of possible combinations of salts and solvents makes it challenging to achieve desirable performance, because even slight variations in composition can lead to noticeable performance degradation. For fast-charging batteries, the need for rapid ionic transport throughout electrolyte to compensate for high current density exacerbates this challenge. This complex transportation problem is strongly correlated with various physical properties of electrolytes, including ionic conductivity, viscosity, diffusivity, and transfer number. These are the problems that need to be solved for better electrolytes. Investigating such a high-dimensional parameter space is impractical using traditional trial-and-error experimentation. Furthermore, since optimal battery design is heavily dependent on application scenarios, identifying optimal electrolytes faces more obstacles.

To tackle this challenge, DL can be useful for accelerating the electrolyte design, both for simulation and experimental approaches. Here we first show some cases for DL-accelerated numerical simulations. Among all simulation methods, molecular dynamic (MD) is the most popular tool to simulate liquid electrolytes. In the electrolyte system, ions lead to a strong local electric field and cause the polarization of the solvent molecules, especially for highly concentrated electrolytes. These polarization terms influence the electrolyte transport properties a lot and therefore need to be predicted by MD [120]. This prediction can be effectively accelerated by implementing NN to learn the atomic polarizabilities and charges [121]. Such an algorithm is only dependent on connectivity of the atoms within a molecule, so the dependencies on the 3D conformation can be avoided. Apart from this, researchers also informed the neural networks with the surrounding environment of the atoms or molecules to improve the accuracy and speed of the prediction (Fig. 9) [122, 123]. These methods offer a widely applicable and automated tool to

comprehend atomic-level dynamics in material systems, considering the vast quantities of molecular dynamics data produced daily in almost all areas of materials design. This provides more insights of the electrolyte properties without completely screening the whole parameter space or synthesizing all possible electrolyte candidates, even in shortage of some physical interactions. To get closer to the cutting-edge battery technologies, highly concentrated electrolyte is more crucial for Zinc ion batteries because it can mitigate the hydrogen evolution reaction. Hence, equivalent methods have been utilized to examine aqueous Zinc electrolyte, which demonstrates that utilizing neural network to learn a functional physical potential is feasible even for extremely disordered systems [124]. They confirmed that the computational results accurately reproduced the observed radial distribution function and X-ray absorption near edge structure spectrum of zinc-water obtained experimentally. There were also other works that demonstrated the implementation of ML in the computational study of electrolytes. Nakayama et al. utilized an exhaustive search with a Gaussian process to gauge the coordination energy [125]. This interaction energy will provide physical insights into the ionic transport of the electrolyte, which is directly related to the performance of fast-charging Li-ion batteries. Moreover, the exhaustive search can also be coupled with linear regression (LiR) to become an ES-LiR model [126]. By using the melting point as a target property for battery operational temperature windows, ES-LiR showed the most accurate estimation compared to MLR and the least absolute shrinkage and selection operator (LASSO) approaches.

Despite the improved accuracy and efficiency of numerical simulation, empirical data plays a crucial role in the battery research domain due to the presence of experimental variations that cannot be adequately described by physical models. Considering this, researchers have begun utilizing ML techniques to facilitate the guidance of electrolyte synthesis experiments. The Cui group at Stanford University employed linear regression, random forest, and bagging models to identify key features for predicting Coulombic efficiency (CE), by utilizing the elemental composition of electrolytes as model features. They created fluorine-free solvent-based electrolyte formulations that achieved a remarkable CE of 99.70% according to the as-trained ML model [49]. The Viswanathan group presented an autonomous method for optimizing battery electrolytes using ML and a robot, where hundreds of sequential experiments were carried out (Fig. 10). A Bayesian optimization technique was employed to explore aqueous electrolyte salt mixtures with excellent electrochemical stability. After conducting 140 electrolyte formula tests over a period of 40 h, an optimal electrolyte, which was not intuitive, is finally obtained [127]. An impressive result is that they presented a dataset of 251 aqueous electrolytes and their conductivities, pH values, and electrochemical reactions on platinum. In the year 2022, a comparable methodology was employed to analyze non-aqueous Li-ion batteries, resulting in a six-fold increase in time efficiency compared to an arbitrary search conducted by the identical automated experiment [128]. In the experimental validation test, it was observed that all the pouch cells that were filled with electrolytes developed by the robot showed improved capability of fast-charging [128]. Their robotic platform, real-time ML optimization, and integration with device testing, tailored to the specific requirement, have the potential to optimize other self-sufficient discovery platforms for energy and sustainability application.

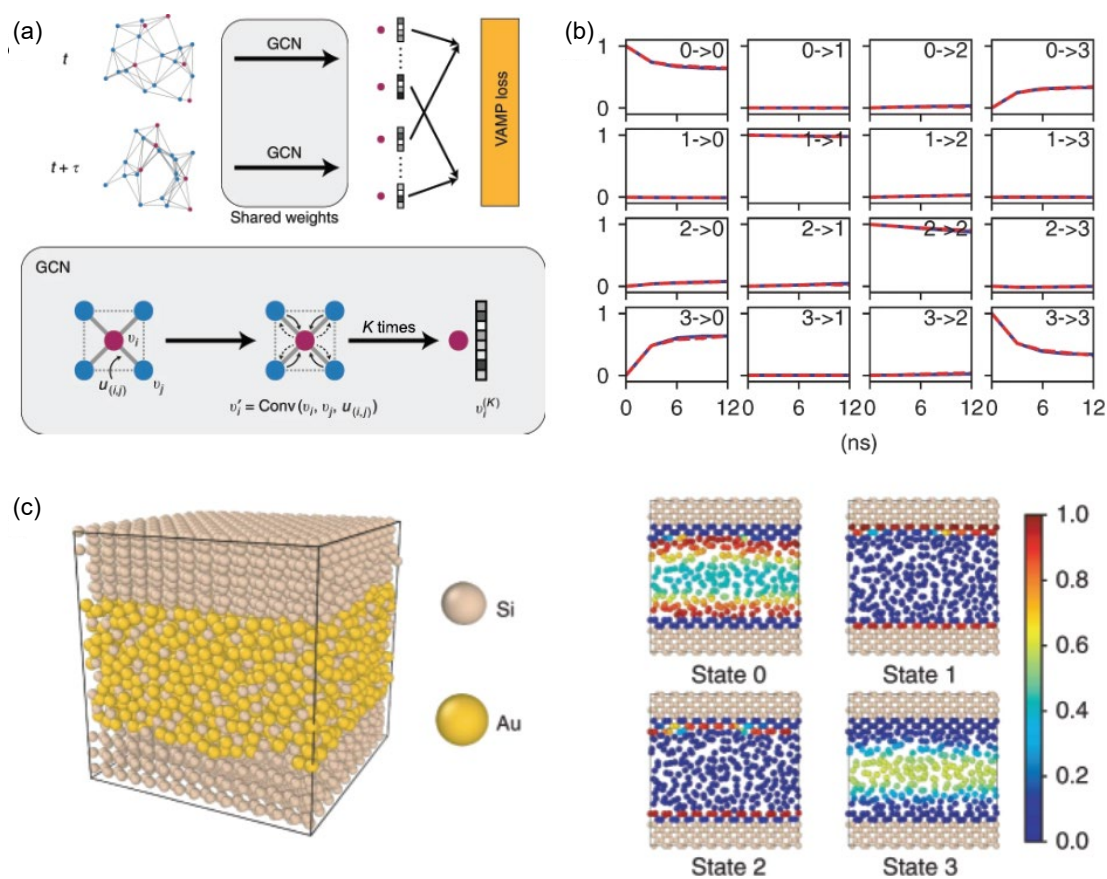


**Figure 9** Graph dynamical networks for unsupervised learning of atomic scale dynamics in materials. (a) Schematics of the graph dynamical networks architecture. (b) Chapman–Kolmogorov (CK) test comparing the long-time dynamics predicted by Koopman models. Reproduced with permission from Ref. [123], © Xie, T. et al. 2019.

In addition to the aforementioned work, there has been substantial progress in designing electrolytes using DL. DL models are instrumental in predicting critical electrolyte properties, including ionic conductivity, viscosity, and stability. These models play a crucial role in pinpointing potential candidate electrolytes tailored for diverse battery chemistries. The molecular Schrödinger equation serves as the fundamental governing principle underlying electrolyte systems. Solving this equation offers detailed insights into chemical reactions occurring within an electric field. Through the utilization of statistical regression models, it has become possible to calculate atomization energies with a remarkably low mean absolute error of approximately 10 kcal/mol [129]. Furthermore, DL, in conjunction with quantum computation, has been employed for the multi-objective optimization of electrolyte compositions. Li et al. outlined a DL workflow integrated with quantum calculations and graph convolutional neural networks to unearth prospective ionic liquids suitable for ionic polymer electrolytes. The predicted electrolyte demonstrated remarkable performance characteristics, including exceptional capacity retention over 350 cycles (> 96% at 0.5 C; > 80% at 2 C), rapid charge/discharge capabilities (146 mAh/g at 3 C), and outstanding efficiency (> 99.92%) [130]. DL also plays a pivotal role in the field of solid-state batteries by facilitating the discovery of optimized solid electrolytes. Sendek et al. conducted a guided exploration of the materials space using a DL-based prediction model for material selection, coupled with density functional theory molecular dynamics (DFT-MD) simulations to compute ionic conductivity. Their findings revealed that the DL-guided search was 2.7 times more likely to identify fast Li-ion conductors, showcasing an impressive improvement of at least

44 times in the log-average of room temperature Li-ion conductivity [131]. This workflow for optimizing solid-state batteries has the potential to identify electrolyte formulations that concurrently enhance battery safety and performance, effectively addressing challenges like dendrite growth and thermal stability.

## 5 Challenges and outlook

Nonetheless, there exist several challenges in the application of DL to battery design. One of the primary hurdles is the availability of high-quality and large-scale data required for training DL models. The creation of comprehensive datasets including diverse battery chemistries, materials, and operating conditions is usually a significant and formidable task. Also, lack of adequate data can lead to overfitting, negatively affecting accuracy. Specifically, battery architectures are often so complex that they require representation with a dimensionality that may exceed the number of samples in the training dataset. Such scenarios can result in poor generalization to unobserved battery architectures, especially when the size of DL model becomes large. Another challenge revolves around model interpretability. DL models, particularly deep neural networks, are frequently perceived as black boxes. In scientific research, understanding the rationale behind a specific prediction of the model is crucial. The development of interpretable DL models for battery design remains a challenge. Transferability is yet another aspect that needs to be improved since battery systems exhibit a high degree of diversity. Models trained on one chemistry or configuration may not easily extend to others. Formulating transferable DL models applicable across different battery types presents a significant challenge.

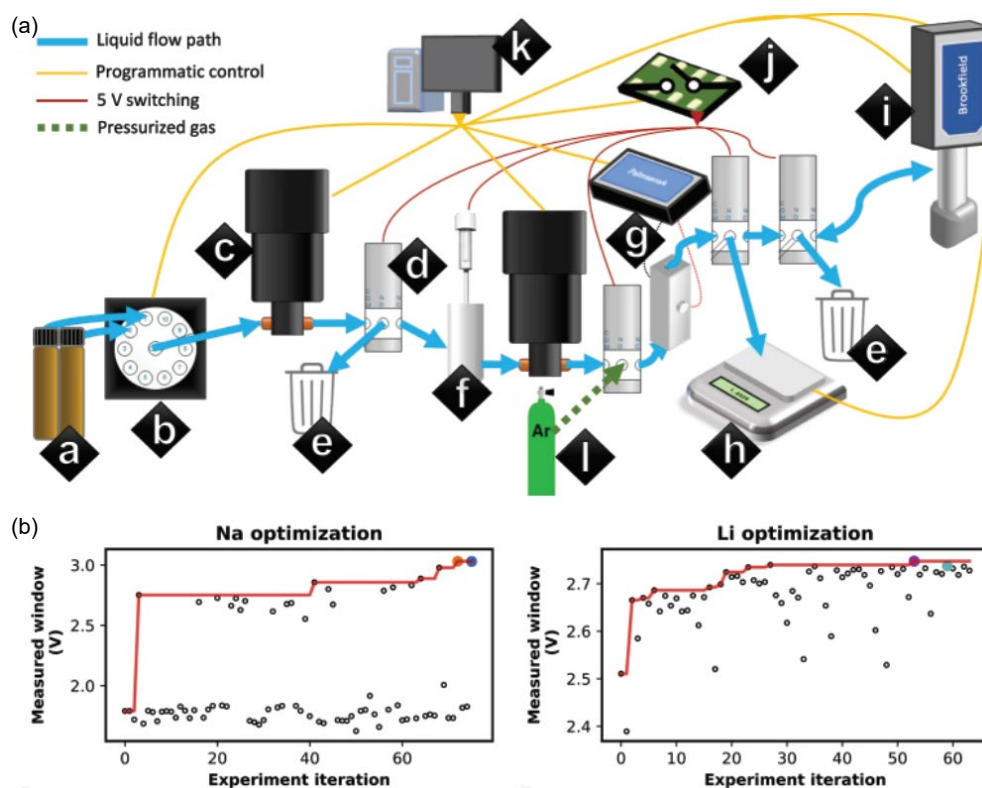


**Figure 10** Autonomous optimization loop for electrolytes. (a) Schematics of automated electrolyte experiment set-up. Reproduced with permission from Ref. [128], © Dave, A. et al. 2022. (b) optimization routine for sodium and lithium electrolytes. Reproduced with permission from Ref. [127], © Dave, A. et al. 2020.

Furthermore, there is an urgent need to reduce the computational cost associated with training a DL model. DL models require substantial computational resources and time for training. Mitigating these resource constraints, particularly for smaller research teams, is pivotal in practice. Last but not least, ensuring data privacy and security is an emerging concern in most battery research endeavors as numerous battery-related datasets contain sensitive information, such as proprietary formulations or experimental details.

Future trends in DL for battery design may prominently feature multi-objective optimization. Researchers are increasingly drawn towards concurrently optimizing multiple properties, including energy density, cycle life, and cost, through the application of deep reinforcement learning. Furthermore, generative models, such as GANs, might be useful for exploring novel battery materials and designs. These models hold the capability to generate new candidates possessing the desired properties, thus potentially expediting innovation. DL models play a guiding role in automated experimentation and robotics platforms. This emerging trend has the potential to accelerate material synthesis and testing, thereby reducing time-to-market for novel battery technologies. Collaborations between diverse specialists, including data scientists, materials scientists, electrochemists, and engineers, are expected to become increasingly popular. Cross-disciplinary teams are essential for effectively addressing the multifaceted challenges in battery design. As the field matures, DL applications in battery design are anticipated to transition from research to integral components of industrial practices. Battery manufacturers and energy companies will progressively harness these tools to drive the development of commercial products. Moreover, battery design will increasingly prioritize sustainability considerations. DL stands to aid in optimizing battery designs with a reduced environmental footprint, encompassing aspects such as recycling and resource utilization.

In short, DL holds immense potential for revolutionizing battery design. Overcoming the challenges associated with data availability, model interpretability, and resource limitations will be important in realizing this potential. The prevailing trends suggest a shift towards more holistic and interdisciplinary approaches, addressing not only performance but also sustainability and efficiency in future battery technologies.

## 6 Conclusions

In conclusion, the application of DL techniques has demonstrated considerable potential to revolutionize the field of battery design. By integrating DL algorithms with traditional experiments and simulations, researchers can accelerate the discovery and characterization of new electrodes and electrolytes, leading to the development of high-performance batteries with improved capacity and cycle life. The combination of accurate first-principle simulation, autonomous synthesis, characterizations, and DL optimization loop has emerged as a promising approach for enhancing the efficiency of battery design and reducing the cost of electric vehicles. Continued exploration of DL algorithms in battery design holds significant promise for advancing the field of materials science, computer science, and engineering to mitigate the impact of climate change.

## Acknowledgments

This work was supported by the startup funding from the Pritzker School of Molecular Engineering, University of Chicago.

## Declaration of conflicting interests

The authors declare no conflicting interests regarding the content of this article.

## Data availability

All data needed to support the conclusions in the paper are presented in the manuscript and/or the Supplementary Materials. Additional data related to this paper may be requested from the corresponding author upon request.

## References

- van Soest, H. L.; den Elzen, M. G. J.; van Vuuren, D. P. Net-zero emission targets for major emitting countries consistent with the Paris Agreement. *Nat. Commun.* **2021**, *12*, 2140.
- United Nations Sustainable Development Goals [Online]. <https://sdgs.un.org/goals> (accessed June 1, 2023).
- Renewable Electricity-Analysis. International Energy Agency [Online]. <https://www.iea.org/reports/renewables-2022/renewable-electricity> (accessed May 10, 2023).
- IEA. *Global EV Outlook 2021*; International Energy Agency: Paris, 2021.
- Nykvist, B.; Nilsson, M. Rapidly falling costs of battery packs for electric vehicles. *Nat. Climate Change* **2015**, *5*, 329–332.
- Deng, W.; Yin, X.; Bao, W.; Zhou, X. F.; Hu, Z. Y.; He, B. Y.; Qiu, B.; Meng, Y. S.; Liu, Z. P. Quantification of reversible and irreversible lithium in practical lithium-metal batteries. *Nat. Energy* **2022**, *7*, 1031–1041.
- Kim, M. S.; Zhang, Z. W.; Wang, J. Y.; Oyakhire, S. T.; Kim, S. C.; Yu, Z. A.; Chen, Y. L.; Boyle, D. T.; Ye, Y. S.; Huang, Z. J. et al. Revealing the multifunctions of Li<sub>3</sub>N in the suspension electrolyte for lithium metal batteries. *ACS Nano* **2023**, *17*, 3168–3180.
- Shimizu, R.; Cheng, D. Y.; Weaver, J. L.; Zhang, M. H.; Lu, B. Y.; Wynn, T. A.; Burger, R.; Kim, M. C.; Zhu, G. M.; Meng, Y. S. Unraveling the stable cathode electrolyte interface in all solid-state thin-film battery operating at 5 V. *Adv. Energy Mater.* **2022**, *12*, 2201119.
- Wang, C. Y.; Liu, T.; Yang, X. G.; Ge, S. H.; Stanley, N. V.; Rountree, E. S.; Leng, Y. J.; McCarthy, B. D. Fast charging of energy-dense lithium-ion batteries. *Nature* **2022**, *611*, 485–490.
- Wang, H. S.; Yu, Z. A.; Kong, X.; Kim, S. C.; Boyle, D. T.; Qin, J.; Bao, Z. N.; Cui, Y. Liquid electrolyte: The nexus of practical lithium metal batteries. *Joule* **2022**, *6*, 588–616.
- Xiao, J.; Shi, F. F.; Glossmann, T.; Burnett, C.; Liu, Z. From laboratory innovations to materials manufacturing for lithium-based batteries. *Nat. Energy* **2023**, *8*, 329–339.
- Zhou, G. M.; Chen, H.; Cui, Y. Formulating energy density for designing practical lithium-sulfur batteries. *Nat. Energy* **2022**, *7*, 312–319.
- Chen, C. B.; Yu, S.; Yang, Y.; Louisia, S.; Roh, I.; Jin, J. B.; Chen, S. P.; Chen, P. C.; Shan, Y.; Yang, P. D. Exploration of the bio-analogous asymmetric C–C coupling mechanism in tandem CO<sub>2</sub> electroreduction. *Nat. Catal.* **2022**, *5*, 878–887.
- Choi, C.; Kwon, S.; Cheng, T.; Xu, M. J.; Tieu, P.; Lee, C.; Cai, J.; Lee, H. M.; Pan, X. Q.; Duan, X. F. et al. Highly active and stable stepped Cu surface for enhanced electrochemical CO<sub>2</sub> reduction to C<sub>2</sub>H<sub>4</sub>. *Nat. Catal.* **2020**, *3*, 804–812.
- Le, D.; Rahman, T. S. On the role of metal cations in CO<sub>2</sub> electrocatalytic reduction. *Nat. Catal.* **2022**, *5*, 977–978.
- Xie, Y.; Ou, P. F.; Wang, X.; Xu, Z. Y.; Li, Y. C.; Wang, Z. Y.; Huang, J. E.; Wicks, J.; McCallum, C.; Wang, N. et al. High carbon utilization in CO<sub>2</sub> reduction to multi-carbon products in acidic media. *Nat. Catal.* **2022**, *5*, 564–570.
- Han, G. Q.; Li, G. D.; Sun, Y. J. Electrocatalytic dual hydrogenation of organic substrates with a Faradaic efficiency approaching 200%. *Nat. Catal.* **2023**, *6*, 224–233.
- Lazaridis, T.; Stühmeier, B. M.; Gasteiger, H. A.; El-Sayed, H. A. Capabilities and limitations of rotating disk electrodes versus membrane electrode assemblies in the investigation of electrocatalysts. *Nat. Catal.* **2022**, *5*, 363–373.
- McCrum, I. T.; Koper, M. T. M. The role of adsorbed hydroxide in hydrogen evolution reaction kinetics on modified platinum. *Nat. Energy* **2020**, *5*, 891–899.
- Tang, B. Y.; Bisbey, R. P.; Lodaya, K. M.; Toh, W. L.; Surendranath, Y. Reaction environment impacts charge transfer but not chemical reaction steps in hydrogen evolution catalysis. *Nat. Catal.* **2023**, *6*, 339–350.
- Sui, C. X.; Hsu, P.-C. Radiative electrochromism for energy-efficient buildings. *Nat. Sustain.* **2023**, *6*, 358–359.
- Barile, C. J.; Slotcavage, D. J.; Hou, J. Y.; Strand, M. T.; Hernandez, T. S.; McGehee, M. D. Dynamic windows with neutral color, high contrast, and excellent durability using reversible metal electrodeposition. *Joule* **2017**, *1*, 133–145.
- Barile, C. J.; Slotcavage, D. J.; McGehee, M. D. Polymer-nanoparticle electrochromic materials that selectively modulate visible and near-infrared light. *Chem. Mater.* **2016**, *28*, 1439–1445.
- Hernandez, T. S.; Barile, C. J.; Strand, M. T.; Dayrit, T. E.; Slotcavage, D. J.; McGehee, M. D. Bistable black electrochromic windows based on the reversible metal electrodeposition of Bi and Cu. *ACS Energy Lett.* **2018**, *3*, 104–111.
- Madu, D. C.; Lilo, M. V.; Thompson, A. A.; Pan, H. Q.; McGehee, M. D.; Barile, C. J. Investigating formate, sulfate, and halide anions in reversible zinc electrodeposition dynamic windows. *ACS Appl. Mater. Interfaces* **2022**, *14*, 47810–47821.
- Sui, C. X.; Pu, J. K.; Chen, T. H.; Liang, J. W.; Lai, Y. T.; Rao, Y. F.; Wu, R. H.; Han, Y.; Wang, K. Y.; Li, X. Q. et al. Dynamic electrochromism for all-season radiative thermoregulation. *Nat. Sustain.* **2023**, *6*, 428–437.
- Nature Sustainability. Research for greener batteries. *Nat. Sustain.* **2021**, *4*, 373.
- Liu, Y. Y.; Zhu, Y. Y.; Cui, Y. Challenges and opportunities towards fast-charging battery materials. *Nat. Energy* **2019**, *4*, 540–550.
- Trahey, L.; Brushett, F. R.; Balsara, N. P.; Ceder, G.; Cheng, L.; Chiang, Y. M.; Hahn, N. T.; Ingram, B. J.; Minter, S. D.; Moore, J. S. et al. Energy storage emerging: A perspective from the Joint Center for Energy Storage Research. *Proc. Natl. Acad. Sci. USA* **2020**, *117*, 12550–12557.
- Ramadesigan, V.; Northrop, P. W. C.; De, S.; Santhanagopalan, S.; Braatz, R. D.; Subramanian, V. R. Modeling and simulation of lithium-ion batteries from a systems engineering perspective. *J. Electrochem. Soc.* **2012**, *159*, R31–R45.
- Agrawal, A.; Choudhary, A. Perspective: Materials informatics and big data: Realization of the “fourth paradigm” of science in materials science. *APL Mater.* **2016**, *4*, 053208.
- Aykol, M.; Hegde, V. I.; Hung, L.; Suram, S.; Herring, P.; Wolverton, C.; Hummelshøj, J. S. Network analysis of synthesizable materials discovery. *Nat. Commun.* **2019**, *10*, 2018.
- Balachandran, P. V.; Kowalski, B.; Sehrioglu, A.; Lookman, T. Experimental search for high-temperature ferroelectric perovskites guided by two-step machine learning. *Nat. Commun.* **2018**, *9*, 1668.
- Butler, K. T.; Davies, D. W.; Cartwright, H.; Isayev, O.; Walsh, A. Machine learning for molecular and materials science. *Nature* **2018**, *559*, 547–555.
- Carrete, J.; Li, W.; Mingo, N.; Wang, S. D.; Curtarolo, S. Finding unprecedentedly low-thermal-conductivity half-Heusler semiconductors via high-throughput materials modeling. *Phys. Rev. X* **2014**, *4*, 011019.
- Coley, C. W.; Jin, W. G.; Rogers, L.; Jamison, T. F.; Jaakkola, T. S.; Green, W. H.; Barzilay, R.; Jensen, K. F. A graph-convolutional neural network model for the prediction of chemical reactivity. *Chem. Sci.* **2019**, *10*, 370–377.
- Granda, J. M.; Donina, L.; Dragone, V.; Long, D. L.; Cronin, L. Controlling an organic synthesis robot with machine learning to search for new reactivity. *Nature* **2018**, *559*, 377–381.
- Isayev, O.; Oses, C.; Toher, C.; Gossett, E.; Curtarolo, S.; Tropsha, A. Universal fragment descriptors for predicting properties of inorganic crystals. *Nat. Commun.* **2017**, *8*, 15679.
- Kim, C.; Pilania, G.; Ramprasad, R. Machine learning assisted

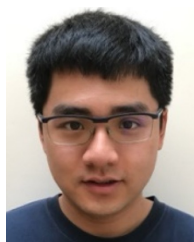
- predictions of intrinsic dielectric breakdown strength of ABX<sub>3</sub> perovskites. *J. Phys. Chem. C* **2016**, *120*, 14575–14580.
- [40] Raccuglia, P.; Elbert, K. C.; Adler, P. D. F.; Falk, C.; Wenny, M. B.; Mollo, A.; Zeller, M.; Friedler, S. A.; Schrier, J.; Norquist, A. J. Machine-learning-assisted materials discovery using failed experiments. *Nature* **2016**, *533*, 73–76.
- [41] Schmidt, J.; Marques, M. R. G.; Botti, S.; Marques, M. A. L. Recent advances and applications of machine learning in solid-state materials science. *npj Comput. Mater.* **2019**, *5*, 83.
- [42] Wang, A. Y. T.; Murdock, R. J.; Kauwe, S. K.; Oliynyk, A. O.; Gurlo, A.; Brgoch, J.; Persson, K. A.; Sparks, T. D. Machine learning for materials scientists: An introductory guide toward best practices. *Chem. Mater.* **2020**, *32*, 4954–4965.
- [43] Ward, L.; Aykol, M.; Blaiszik, B.; Foster, I.; Meredig, B.; Saal, J.; Suram, S. Strategies for accelerating the adoption of materials informatics. *MRS Bull.* **2018**, *43*, 683–689.
- [44] Xue, D. Z.; Balachandran, P. V.; Hogden, J.; Theiler, J.; Xue, D. Q.; Lookman, T. Accelerated search for materials with targeted properties by adaptive design. *Nat. Commun.* **2016**, *7*, 11241.
- [45] Schütt, K. T.; Arbabzadah, F.; Chmiela, S.; Müller, K. R.; Tkatchenko, A. Quantum-chemical insights from deep tensor neural networks. *Nat. Commun.* **2017**, *8*, 13890.
- [46] Attia, P. M.; Grover, A.; Jin, N.; Severson, K. A.; Markov, T. M.; Liao, Y. H.; Chen, M. H.; Cheong, B.; Perkins, N.; Yang, Z. et al. Closed-loop optimization of fast-charging protocols for batteries with machine learning. *Nature* **2020**, *578*, 397–402.
- [47] Severson, K. A.; Attia, P. M.; Jin, N.; Perkins, N.; Jiang, B. B.; Yang, Z.; Chen, M. H.; Aykol, M.; Herring, P. K.; Fragedakis, D. et al. Data-driven prediction of battery cycle life before capacity degradation. *Nat. Energy* **2019**, *4*, 383–391.
- [48] Bhowmik, A.; Castelli, I. E.; Garcia-Lastra, J. M.; Jørgensen, P. B.; Winther, O.; Vegge, T. A perspective on inverse design of battery interphases using multi-scale modelling, experiments and generative deep learning. *Energy Storage Mater.* **2019**, *21*, 446–456.
- [49] Kim, S. C.; Oyakhire, S. T.; Athanitis, C.; Wang, J. Y.; Zhang, Z. W.; Zhang, W. B.; Boyle, D. T.; Kim, M. S.; Yu, Z. A.; Gao, X. et al. Data-driven electrolyte design for lithium metal anodes. *Proc. Natl. Acad. Sci. USA* **2023**, *120*, e2214357120.
- [50] Zhang, D. W.; Zhong, C.; Xu, P. J.; Tian, Y. Y. Deep learning in the state of charge estimation for Li-ion batteries of electric vehicles: A review. *Machines* **2022**, *10*, 912.
- [51] Scharf, J.; Chouchane, M.; Finegan, D. P.; Lu, B. Y.; Redquest, C.; Kim, M. C.; Yao, W. L.; Franco, A. A.; Gostovic, D.; Liu, Z. et al. Bridging nano-and microscale X-ray tomography for battery research by leveraging artificial intelligence. *Nat. Nanotechnol.* **2022**, *17*, 446–459.
- [52] Bishop, C. M. *Pattern Recognition and Machine Learning*; Springer: New York, 2006.
- [53] Rudin, C.; Carlson, D. The secrets of machine learning: Ten things you wish you had known earlier to be more effective at data analysis. In *Proceedings of the Operations Research & Management Science in the Age of Analytics*, Catonsville, USA, 2019, pp 44–72.
- [54] Drucker, H.; Burges, C. J. C.; Kaufman, L.; Smola, A.; Vapnik, V. Support vector regression machines. In *Proceedings of the 9<sup>th</sup> International Conference on Neural Information Processing Systems*, Denver, USA, 1996, pp 155–161.
- [55] Hoerl, A. E.; Kennard, R. W. Ridge regression: Biased estimation for nonorthogonal problems. *Technometrics* **1970**, *12*, 55–67.
- [56] Tibshirani, R. Regression shrinkage and selection via the lasso. *J. Roy. Stat. Soc.: Ser. B Methodol.* **1996**, *58*, 267–288.
- [57] Rasmussen, C. E.; Williams, C. K. I. *Model Selection and Adaptation of Hyperparameters*; MIT Press: Cambridge, 2005.
- [58] Jiang, Z. Y.; Zheng, T. S.; Liu, Y. L.; Carlson, D. Incorporating prior knowledge into neural networks through an implicit composite kernel. 2022, arXiv preprint arXiv:2205.07384. arXiv.org e-Print archive. <https://doi.org/10.48550/arXiv.2205.07384> (accessed May 12, 2023).
- [59] Frazier, P. I. A tutorial on bayesian optimization. 2018, arXiv:1807.02811. arXiv.org e-Print archive. <https://doi.org/10.48550/arXiv.1807.02811> (accessed May 11, 2023).
- [60] Snoek, J.; Larochelle, H.; Adams, R. P. Practical bayesian optimization of machine learning algorithms. In *Proceedings of the 25<sup>th</sup> International Conference on Neural Information Processing Systems*, Lake Tahoe, USA, 2012, pp 2951–2959.
- [61] LeCun, Y.; Bengio, Y.; Hinton, G. Deep learning. *Nature* **2015**, *521*, 436–444.
- [62] Lin, Y.; Dong, H. Z.; Wang, H.; Zhang, T. Bayesian invariant risk minimization. In *Proceedings of 2022 IEEE/CVF Conference on Computer Vision and Pattern Recognition*, New Orleans, USA, 2022, pp 16000–16009.
- [63] Ramesh, A.; Pavlov, M.; Goh, G.; Gray, S.; Voss, C.; Radford, A.; Chen, M.; Sutskever, I. Zero-shot text-to-image generation. In *Proceedings of the 38<sup>th</sup> International Conference on Machine Learning*, Virtual, 18–24 July 2021, pp 8821–8831.
- [64] Sohl-Dickstein, J.; Weiss, E. A.; Maheswaranathan, N.; Ganguli, S. Deep unsupervised learning using nonequilibrium thermodynamics. In *Proceedings of the 32<sup>nd</sup> International Conference on Machine Learning*, Lille, France, 2015, pp 2256–2265.
- [65] Brown, T. B.; Mann, B.; Ryder, N.; Subbiah, M.; Kaplan, J.; Dhariwal, P.; Neelakantan, A.; Shyam, P.; Sastry, G.; Askell, A. et al. Language models are few-shot learners. In *Proceedings of the 34<sup>th</sup> International Conference on Neural Information Processing Systems*, Vancouver, Canada, 2020, pp 159.
- [66] Devlin, J.; Chang, M. W.; Lee, K.; Toutanova, K. BERT: Pre-training of deep bidirectional transformers for language understanding. In *Proceedings of the 2019 Conference of the North American Chapter of the Association for Computational Linguistics: Human Language Technologies*, Minneapolis, USA, 2018, pp 4171–4186.
- [67] Vaswani, A.; Shazeer, N.; Parmar, N.; Uszkoreit, J.; Jones, L.; Gomez, A. N.; Kaiser, Ł.; Polosukhin, I. Attention is all you need. In *Proceedings of the 31<sup>st</sup> International Conference on Neural Information Processing Systems*, Long Beach, USA, 2017, pp 6000–6010.
- [68] Hatt, T.; Feuerriegel, S. Estimating average treatment effects via orthogonal regularization. In *Proceedings of the 30<sup>th</sup> ACM International Conference on Information & Knowledge Management*, Queensland, Australia, 2021, pp 680–689.
- [69] Jiang, Z. Y.; Hou, Z. R.; Liu, Y. L.; Ren, Y. M.; Li, K. Y.; Carlson, D. E. Estimating causal effects using a multi-task deep ensemble. In *Proceedings of the International Conference on Machine Learning*, Honolulu, USA, 2023, pp 15023–15040.
- [70] Louizos, C.; Shalit, U.; Mooij, J.; Sontag, D.; Zemel, R.; Welling, M. Causal effect inference with deep latent-variable models. In *Proceedings of the 31<sup>st</sup> International Conference on Neural Information Processing Systems*, Long Beach, USA, 2017, pp 6449–6459.
- [71] Shalit, U.; Johansson, F. D.; Sontag, D. Estimating individual treatment effect: Generalization bounds and algorithms. In *Proceedings of the 34<sup>th</sup> International Conference on Machine Learning*, Sydney, Australia, 2017, pp 3076–3085.
- [72] Jiang, Z. Y.; Liu, Y. L.; Klein, M. H.; Aloui, A.; Ren, Y. M.; Li, K. Y.; Tarokh, V.; Carlson, D. Causal mediation analysis with multi-dimensional and indirectly observed mediators. 2023, arXiv:2306.07918. arXiv.org e-Print archive. <https://arxiv.org/abs/2306.07918> (accessed April 20, 2023).
- [73] Ahmad, M. A.; Eckert, C.; Teredesai, A. Interpretable machine learning in healthcare. In *Proceedings of the 2018 ACM International Conference on Bioinformatics, Computational Biology, and Health Informatics*, Washington, DC, USA, 2018, pp 559–560.
- [74] Erickson, B. J.; Korfiatis, P.; Akkus, Z.; Kline, T. L. Machine learning for medical imaging. *Radiographics* **2017**, *37*, 505–515.
- [75] Miotto, R.; Wang, F.; Wang, S.; Jiang, X. Q.; Dudley, J. T. Deep learning for healthcare: Review, opportunities and challenges. *Brief. Bioinform.* **2018**, *19*, 1236–1246.

- [76] Jiang, Z. Y.; Zheng, T. S.; Bergin, M.; Carlson, D. Improving spatial variation of ground-level PM<sub>2.5</sub> prediction with contrastive learning from satellite imagery. *Sci. Remote Sens.* **2022**, *5*, 100052.
- [77] Zheng, T. S.; Bergin, M.; Wang, G. Y.; Carlson, D. Local PM<sub>2.5</sub> hotspot detector at 300 m resolution: A random forest-convolutional neural network joint model jointly trained on satellite images and meteorology. *Remote Sens.* **2021**, *13*, 1356.
- [78] Zheng, T. S.; Bergin, M. H.; Hu, S. J.; Miller, J.; Carlson, D. E. Estimating ground-level PM<sub>2.5</sub> using micro-satellite images by a convolutional neural network and random forest approach. *Atmos. Environ.* **2020**, *230*, 117451.
- [79] Agarap, A. F. Deep learning using rectified linear units (ReLU). 2018, arXiv:1803.08375. arXiv.org e-Print archive. <https://doi.org/10.48550/arXiv.1803.08375> (accessed April 1, 2023).
- [80] Maas, A. L.; Hannun, A. Y.; Ng, A. Y. Rectifier nonlinearities improve neural network acoustic models. In *Proceedings of the 30<sup>th</sup> International Conference on Machine Learning*, Atlanta, USA, 2013, pp 3.
- [81] Karlik, B.; Vehbi, A. Performance analysis of various activation functions in generalized MLP architectures of neural networks. *Int. J. Artif. Intell. Expert Syst.* **2011**, *1*, 111–122.
- [82] Rumelhart, D. E.; Hinton, G. E.; Williams, R. J. Learning representations by back-propagating errors. *Nature* **1986**, *323*, 533–536.
- [83] Le Cun, Y.; Jackel, L. D.; Boser, B.; Denker, J. S.; Graf, H. P.; Guyon, I.; Henderson, D.; Howard, R. E.; Hubbard, W. Handwritten digit recognition: Applications of neural network chips and automatic learning. *IEEE Commun. Mag.* **1989**, *27*, 41–46.
- [84] LeCun, Y.; Bengio, Y. Convolutional networks for images, speech, and time-series. In *Proceedings of the Handbook of Brain Theory and Neural Networks*, Cambridge, USA, 1998, pp 255–258.
- [85] Jordan, M. I. Serial order: A parallel distributed processing approach. *Adv. Psychol.* **1997**, *121*, 471–495.
- [86] Werbos, P. J. Backpropagation through time: What it does and how to do it. *Proc. IEEE* **1990**, *78*, 1550–1560.
- [87] Hochreiter, S.; Schmidhuber, J. Long short-term memory. *Neural Comput.* **1997**, *9*, 1735–1780.
- [88] Chung, J.; Gulcehre, C.; Cho, K.; Bengio, Y. Empirical evaluation of gated recurrent neural networks on sequence modeling. 2014, arXiv:1412.3555. arXiv.org e-Print archive. <https://doi.org/10.48550/arXiv.1412.3555> (accessed March 19, 2023).
- [89] Jozefowicz, R.; Zaremba, W.; Sutskever, I. An empirical exploration of recurrent network architectures. In *Proceedings of the 32<sup>nd</sup> International Conference on Machine Learning*, Lille, France, 2015, pp 2342–2350.
- [90] Bahdanau, D.; Cho, K.; Bengio, Y. Neural machine translation by jointly learning to align and translate. In *Proceedings of the 3<sup>rd</sup> International Conference on Learning Representations*, San Diego, USA, 2015.
- [91] Masci, J.; Meier, U.; Cireşan, D.; Schmidhuber, J. Stacked convolutional auto-encoders for hierarchical feature extraction. In *Proceedings of the 21<sup>st</sup> International Conference on Artificial Neural Networks*, Espoo, Finland, 2011, pp 52–59.
- [92] Kingma, D. P.; Welling, M. Auto-encoding variational bayes. In *Proceedings of the 2<sup>nd</sup> International Conference on Learning Representations*, Banff, Canada, 2014.
- [93] Goodfellow, I.; Pouget-Abadie, J.; Mirza, M.; Xu, B.; Warde-Farley, D.; Ozair, S.; Courville, A.; Bengio, Y. Generative adversarial networks. *Commun. ACM* **2020**, *63*, 139–144.
- [94] Arora, S.; Risteski, A.; Zhang, Y. Do GANs learn the distribution? Some theory and empirics. In *Proceedings of the 6<sup>th</sup> International Conference on Learning Representations*, Vancouver, Canada, 2018.
- [95] Ho, J.; Jain, A.; Abbeel, P. Denoising diffusion probabilistic models. In *Proceedings of the 34<sup>th</sup> International Conference on Neural Information Processing Systems*, Vancouver, Canada, 2020, pp 574.
- [96] Bond-Taylor, S.; Leach, A.; Long, Y.; Willcocks, C. G. Deep generative modelling: A comparative review of vaes, gans, normalizing flows, energy-based and autoregressive models. *IEEE Trans. Pattern Anal. Mach. Intell.* **2022**, *44*, 7327–7347.
- [97] Sui, C. X.; Li, Y. Y.; Li, X. Q.; Higueros, G.; Wang, K. Y.; Xie, W. R.; Hsu, P. C. Bio-inspired computational design of vascularized electrodes for high-performance fast-charging batteries optimized by deep learning. *Adv. Energy Mater.* **2022**, *12*, 2103044.
- [98] Newman, J.; Balsara, N. P. *Electrochemical Systems*, 4<sup>th</sup> ed.; John Wiley & Sons: New York, 2021.
- [99] Li, L. S.; Erb, R. M.; Wang, J. J.; Wang, J.; Chiang, Y. M. Fabrication of low-tortuosity ultrahigh-area-capacity battery electrodes through magnetic alignment of emulsion-based slurries. *Adv. Energy Mater.* **2019**, *9*, 1802472.
- [100] Wu, J. Y.; Ju, Z. Y.; Zhang, X.; Xu, X.; Takeuchi, K. J.; Marschilok, A. C.; Takeuchi, E. S.; Yu, G. H. Low-tortuosity thick electrodes with active materials gradient design for enhanced energy storage. *ACS Nano* **2022**, *16*, 4805–4812.
- [101] Qi, Y. B.; Jang, T. J.; Ramadesigan, V.; Schwartz, D. T.; Subramanian, V. R. Is there a benefit in employing graded electrodes for lithium-ion batteries? *J. Electrochem. Soc.* **2017**, *164*, A3196–A3207.
- [102] Ramadesigan, V.; Methekar, R. N.; Latinwo, F.; Braatz, R. D.; Subramanian, V. R. Optimal porosity distribution for minimized ohmic drop across a porous electrode. *J. Electrochem. Soc.* **2010**, *157*, A1328.
- [103] Liu, L.; Guan, P. J.; Liu, C. H. Experimental and simulation investigations of porosity graded cathodes in mitigating battery degradation of high voltage lithium-ion batteries. *J. Electrochem. Soc.* **2017**, *164*, A3163–A3173.
- [104] Zhang, X.; Hui, Z. Y.; King, S. T.; Wu, J. Y.; Ju, Z. Y.; Takeuchi, K. J.; Marschilok, A. C.; West, A. C.; Takeuchi, E. S.; Wang, L. et al. Gradient architecture design in scalable porous battery electrodes. *Nano Lett.* **2022**, *22*, 2521–2528.
- [105] Huang, C.; Dontigny, M.; Zaghbi, K.; Grant, P. S. Low-tortuosity and graded lithium ion battery cathodes by ice templating. *J. Mater. Chem. A* **2019**, *7*, 21421–21431.
- [106] Kim, H.; Oh, S. K.; Lee, J.; Doo, S. W.; Kim, Y.; Lee, K. T. Failure mode of thick cathodes for Li-ion batteries: Variation of state-of-charge along the electrode thickness direction. *Electrochim. Acta* **2021**, *370*, 137743.
- [107] Bae, C. J.; Erdonmez, C. K.; Halloran, J. W.; Chiang, Y. M. Design of battery electrodes with dual-scale porosity to minimize tortuosity and maximize performance. *Adv. Mater.* **2013**, *25*, 1254–1258.
- [108] Sander, J. S.; Erb, R. M.; Li, L.; Gurijala, A.; Chiang, Y. M. High-performance battery electrodes via magnetic templating. *Nat. Energy* **2016**, *1*, 16099.
- [109] Billaud, J.; Bouville, F.; Magrini, T.; Villeveille, C.; Studart, A. R. Magnetically aligned graphite electrodes for high-rate performance Li-ion batteries. *Nat. Energy* **2016**, *1*, 16097.
- [110] Zhang, X.; Ju, Z. Y.; Housel, L. M.; Wang, L.; Zhu, Y.; Singh, G.; Sadique, N.; Takeuchi, K. J.; Takeuchi, E. S.; Marschilok, A. C. et al. Promoting transport kinetics in Li-ion battery with aligned porous electrode architectures. *Nano Lett.* **2019**, *19*, 8255–8261.
- [111] Xu, T. Topology optimization of lithium ion batteries: How to maximize the discharge capacity by changing the geometry. Master thesis, Delft University of Technology, Delft, 2015.
- [112] Niu, Z. Q.; Zhao, W. H.; Wu, B.; Wang, H. Z.; Lin, W. F.; Pinfield, V. J.; Xuan, J.  $\pi$  Learning: A performance-informed framework for microstructural electrode design. *Adv. Energy Mater.* **2023**, *13*, 2300244.
- [113] Arganda-Carreras, I.; Kaynig, V.; Rueden, C.; Eliceiri, K. W.; Schindelin, J.; Cardona, A.; Sebastian Seung, H. Trainable Weka Segmentation: A machine learning tool for microscopy pixel classification. *Bioinformatics* **2017**, *33*, 2424–2426.
- [114] Chan, H. P.; Samala, R. K.; Hadjiiski, L. M.; Zhou, C. Deep learning in medical image analysis. In *Deep Learning in Medical Image Analysis: Challenges and Applications*. Lee, G.; Fujita, H., Eds.; Springer: Cham, 2020; pp 3–21.

- [115] Kench, S.; Cooper, S. J. Generating three-dimensional structures from a two-dimensional slice with generative adversarial network-based dimensionality expansion. *Nat. Mach. Intell.* **2021**, *3*, 299–305.
- [116] Xu, H. Y.; Zhu, J. E.; Finegan, D. P.; Zhao, H. B.; Lu, X. K.; Li, W.; Hoffman, N.; Bertei, A.; Shearing, P.; Bazant, M. Z. Guiding the design of heterogeneous electrode microstructures for Li-ion batteries: Microscopic imaging, predictive modeling, and machine learning. *Adv. Energy Mater.* **2021**, *11*, 2003908.
- [117] Yang, Y. Z.; Li, N.; Wang, B.; Li, N.; Gao, K.; Liang, Y. D.; Wei, Y. M.; Yang, L.; Song, W. L.; Chen, H. S. Microstructure evolution of lithium-ion battery electrodes at different states of charge: Deep learning-based segmentation. *Electrochem. Commun.* **2022**, *136*, 107224.
- [118] Gayon-Lombardo, A.; Mosser, L.; Brandon, N. P.; Cooper, S. J. Pores for thought: Generative adversarial networks for stochastic reconstruction of 3D multi-phase electrode microstructures with periodic boundaries. *npj Comput. Mater.* **2020**, *6*, 82.
- [119] Petrich, L.; Westhoff, D.; Feinauer, J.; Finegan, D. P.; Daemi, S. R.; Shearing, P. R.; Schmidt, V. Crack detection in lithium-ion cells using machine learning. *Comput. Mater. Sci.* **2017**, *136*, 297–305.
- [120] Bedrov, D.; Piquemal, J. P.; Borodin, O.; Mackerell, A. D.; Roux, B.; Schröder, C. Molecular dynamics simulations of ionic liquids and electrolytes using polarizable force fields. *Chem. Rev.* **2019**, *119*, 7940–7995.
- [121] Heid, E.; Fleck, M.; Chatterjee, P.; Schröder, C.; MacKerell, A. D. Jr. Toward prediction of electrostatic parameters for force fields that explicitly treat electronic polarization. *J. Chem. Theory Comput.* **2019**, *15*, 2460–2469.
- [122] Schütt, K. T.; Sauceda, H. E.; Kindermans, P. J.; Tkatchenko, A.; Müller, K. R. SchNet—A deep learning architecture for molecules and materials. *J. Chem. Phys.* **2018**, *148*, 241722.
- [123] Xie, T.; France-Lanord, A.; Wang, Y. M.; Shao-Horn, Y.; Grossman, J. C. Graph dynamical networks for unsupervised learning of atomic scale dynamics in materials. *Nat. Commun.* **2019**, *10*, 2667.
- [124] Xu, M. Y.; Zhu, T.; Zhang, J. Z. H. Molecular dynamics simulation of zinc ion in water with an *ab initio* based neural network potential. *J. Phys. Chem A* **2019**, *123*, 6587–6595.
- [125] Nakayama, T.; Igarashi, Y.; Sodeyama, K.; Okada, M. Material search for Li-ion battery electrolytes through an exhaustive search with a Gaussian process. *Chem. Phys. Lett.* **2019**, *731*, 136622.
- [126] Sodeyama, K.; Igarashi, Y.; Nakayama, T.; Tateyama, Y.; Okada, M. Liquid electrolyte informatics using an exhaustive search with linear regression. *Phys. Chem. Chem. Phys.* **2018**, *20*, 22585–22591.
- [127] Dave, A.; Mitchell, J.; Kandasamy, K.; Wang, H.; Burke, S.; Paria, B.; Póczos, B.; Whitacre, J.; Viswanathan, V. Autonomous discovery of battery electrolytes with robotic experimentation and machine learning. *Cell Rep. Phys. Sci.* **2020**, *1*, 100264.
- [128] Dave, A.; Mitchell, J.; Burke, S.; Lin, H. Y.; Whitacre, J.; Viswanathan, V. Autonomous optimization of non-aqueous Li-ion battery electrolytes via robotic experimentation and machine learning coupling. *Nat. Commun.* **2022**, *13*, 5454.
- [129] Rupp, M.; Tkatchenko, A.; Müller, K. R.; von Lilienfeld, O. A. Fast and accurate modeling of molecular atomization energies with machine learning. *Phys. Rev. Lett.* **2012**, *108*, 058301.
- [130] Li, K.; Wang, J. F.; Song, Y. Y.; Wang, Y. Machine learning-guided discovery of ionic polymer electrolytes for lithium metal batteries. *Nat. Commun.* **2023**, *14*, 2789.
- [131] Sendek, A. D.; Cubuk, E. D.; Antoniuk, E. R.; Cheon, G.; Cui, Y.; Reed, E. J. Machine learning-assisted discovery of solid Li-ion conducting materials. *Chem. Mater.* **2019**, *31*, 342–352.



**Chenxi Sui** received his B.S. degree in physics from Wuhan University. He is now a Ph.D. candidate at the University of Chicago, majoring in molecular engineering. His research focus on experimental and computational study on electrochemistry, heat transfer, photonics and deep learning. He has published several papers on *Nature Sustainability*, *Nature Communication*, *Science Advances*, *Advanced Energy Materials* and *ACS Energy Letters*.



**Ziyang Jiang** received his Master's degree in Civil and Environmental Engineering from Stanford University in 2019. He is currently a Ph.D. candidate under the supervision of Prof. David Carlson at Duke University. His research interest focuses on developing methodologies for integrating domain knowledge in the environmental and healthcare data with deep learning models, thus improving their generalization capability in specific applications such as air pollution spatial mapping and causal inference for clinical trials.



**Genesis Higueros** is a fifth year Ph.D. candidate in Mechanical Engineering and Materials Science at Duke University. Her research focuses on radiative shielding textiles and fast-charging novel 3D electrode materials. She is also an Alfred P. Sloan 2019-23 Scholar. Genesis received a Bachelor of Science in Environmental Engineering, Highest Honors, from the University of California, Merced. Genesis also organizes STEM outreach programs for students from underrepresented communities.



**David Carlson** received the B.S.E., M.S., and Ph.D. degrees from Duke University, Durham, NC, USA, in 2010, 2014, and 2015, respectively. He completed Postdoctoral Training with the Department of Statistics at Columbia University, New York, NY, USA. He is currently an Assistant Professor of civil and environmental engineering, biostatistics and bioinformatics, electrical and computer engineering, and computer science. His research focus is on developing novel machine learning and artificial intelligence techniques that can be used to accelerate scientific discovery. Additionally, he has multiple partnerships deploying machine learning techniques for applications in environmental health, mental health, and neuroscience.



**Po-Chun Hsu** is an Assistant Professor at the Pritzker School of Molecular Engineering at the University of Chicago. Prof. Hsu received his B.S. degree from National Tsing Hua University. He earned his Ph.D. degree in Materials Science and Engineering and was a postdoctoral researcher in Mechanical Engineering, both at Stanford University.